

Supplementary Information

Multifunctional near-infrared laser-triggered drug delivery system using folic acid conjugated chitosan oligosaccharide encapsulated gold nanorods for targeted chemo-photothermal therapy

Panchanathan Manivasagan,^{a1} Seung Won Jun,^{b1} Van Tu Nguyen,^c Phong Truong Nguyen Thanh,^c Giang Hoang,^a Sudip Mondal,^a Madhappan Santha Moorthy,^a Hye Hyun Kim,^a Thi Tuong Vy Phan,^c Vu Hoang Minh Doan,^c Chang-Seok Kim,^{*b} Junghwan Oh ^{*ac}

^a Marine-Integrated Bionics Research Center, Pukyong National University, Busan 48513, Republic of Korea.

^b Department of Cogno-Mechatronics Engineering, Pusan National University, Busan 46241, Republic of Korea.

^c Department of Biomedical Engineering and Center for Marine-Integrated Biotechnology (BK21 Plus), Pukyong National University, Busan 48513, Republic of Korea.

¹ These authors contributed equally to this work

*** Corresponding author: Prof. Junghwan Oh ^{*ac} and Prof. Chang-Seok Kim ^{*b}**

^a Marine-Integrated Bionics Research Center, Pukyong National University, Busan 48513, Republic of Korea.

^c Department of Biomedical Engineering and Center for Marine-Integrated Biotechnology (BK21 Plus), Pukyong National University, Busan 48513, Republic of Korea.

Email: jungoh@pknu.ac.kr; Tel: +82-51-629-5771, Fax: +82-51-629-5779.

^b Department of Cogno-Mechatronics Engineering, Pusan National University, Busan 46241, Republic of Korea. Email: ckim@pusan.ac.kr; Tel: +82-51-510-1365.

Experimental

Materials and methods

Materials

All reagents and materials were obtained from Sigma-Aldrich and were used as received without further purification.

Preparation of FA-COS-TGA-GNRs-DOX

Folic acid-chitosan oligosaccharide (FA-COS) was prepared according to earlier works ^{1,2}. 0.11 g of FA (0.25 mM) was completely dissolved in 10 mL dehydrated dimethyl sulfoxide (DMSO), and the carboxyl groups of the FA solution were activated by 0.2 g of 1-ethyl-3-(3-dimethyl aminopropyl) carbodiimide (EDC; 0.5 mM) and 0.05 g of N-hydroxysuccinimide (NHS; 0.3 mM) at ambient temperature in the dark for 40 min. The free amino groups of COS (0.4 g, 0.1 mM; M_n = 5000 Da, 90% deacetylated degree) were conjugated with the carboxyl groups of FA in the presence of EDC/NHS as a catalyst, and COS was added to the FA solution at ambient temperature in the dark for 24 h. The reaction solution was filtered, washed with distilled water three times and ethanol alternatively to remove unbound molecules, and freeze-dried. FA-COS was further encapsulated with thioglycolic acid (TGA) via a coupling reaction with the carboxyl groups of TGA in the presence of EDC/NHS. 3.251 g of FA-COS, 1.542 g of EDC, and 0.683 g of NHS were dissolved in 50 mL of deionized water. 0.573 g of 2 mM TGA was added into the FA-COS solution, and the solution was stirred for 24 h. The resultants were dialyzed against deionized water using a dialysis membrane (MWCO: 3500 Da) for 5 days and freeze dried. The structure of FA-

COS and FA-COS-TGA were characterized by ^1H NMR. The ^1H NMR spectra were obtained in D_2O using a JNM ECP-400 (400 MHz, JEOL, Japan) spectrometer.

Gold nanorods (GNRs) were also synthesized according to earlier works ³⁻⁶. For the encapsulation process of GNRs, 5 g of FA-COS-TGA was added in 10 mL of purified GNRs through gold–thiol interaction and allowed to react at ambient temperature for 24 h ⁷. The encapsulated GNRs (FA-COS-TGA-GNRs) were purified by centrifugation and washed more than three times with deionized water. For the hydrolysis of COS, 5 mL of FA-COS-TGA-GNRs and 0.1 M sodium hydroxide (NaOH) were added to hydrolyze the pyromellitic dianhydride (PMDA) under basic medium ⁸. The solution was stirred at 50 °C for 30 min, and the reaction solution (FA-COS-TGA-GNRs-PMDA) was purified by centrifugation and subsequent re-dispersion into the deionized water. The DOX molecules were loaded onto FA-COS-TGA-GNRs-PMDA via the possible physical interactions specifically, H-bonding/electrostatic interaction between the carboxyl acid group of PMDA and the amine groups of DOX molecules ⁹. Briefly, 0.3 mL of DOX solution at a concentration of 1 mg mL⁻¹ (pH 7.4) was added into 10 mL of FA-COS-TGA-GNRs-PMDA (1 mg mL⁻¹) dispersion and stirred for 24 h to allow the DOX-loading process to reach equilibrium. Then, the FA-COS-TGA-GNRs-PMDA-DOX solution was dialyzed against deionized water (pH. 7.4) to remove unreacted DOX. The obtained purified folic acid conjugated and doxorubicin-loaded chitosan oligosaccharide encapsulated gold nanorods (FA-COS-TGA-GNRs-DOX) were dispersed in phosphate-buffered saline (PBS) for further characterization and biomedical applications. The substitution degree of amino groups was measured using the 2,4,6-trinitrobenzene sulfonic acid (TNBS) technique.

***In vitro* drug release test**

The dispersion was centrifuged at 15,000 rpm for 10 min to collect FA-COS-TGA-GNRs-DOX, and the supernatant was used to determine the drug loading content. The DOX concentration in the supernatant was determined by measuring the absorbance of the drug at 480 nm using a UV-vis spectrophotometer. The drug loading content and entrapment efficiency were calculated using the following equations:

$$\text{Drug loading content} = \frac{\text{Weight of drug in nanoparticles (NPs)}}{\text{Weight of NPs}} \times 100$$

$$\text{Drug entrapment efficiency} = \frac{\text{Weight of drug in NPs}}{\text{Weight of drug fed initially}} \times 100$$

***In vitro* NIR laser-triggered release of DOX from FA-COS-TGA-GNRs-DOX**

In vitro NIR laser-triggered drug release studies were performed in various pH buffers (5.0 and 7.4) at room temperature with the same mass concentration. Briefly, 5 mg of FA-COS-TGA-GNRs-DOX was redispersed in PBS and was exposed to an 808 nm laser (1.0 W cm⁻²) for 300 s. The drug release efficiency was quantified using a UV-vis spectrophotometer at 480 nm at various time intervals and was calculated using the following equation:

$$\text{Cumulative drug release} = \frac{\text{Weight of drug in the supernatant by the following equation}}{\text{Entrapment of efficiency of FA - COS - TGA - GNRs - DOX}} \times 100$$

Instrumentation

Sample morphology and structure were observed using a JEM-1010 (JEOL, Japan) high-resolution transmission electron microscopy (HRTEM) and selected area electron diffraction (SAED) pattern. TEM was also used for energy dispersive X-ray spectroscopy (EDX). Ultraviolet-visible-near infrared (UV-vis-NIR) spectra were evaluated in the wavelength range of 400–1000 nm using a Genesys 30S UV-vis spectrophotometer (Thermo Scientific, USA). Dynamic light scattering (DLS) and zeta potential (ZP) measurement were performed using an ELS-8000

electrophoretic light scattering spectrophotometer (Otsuka, Electronics Co. Ltd., Japan). The Fourier-transform infrared (FTIR) spectra were measured on a Perkin-Elmer Spectrum 100 FTIR spectrometer (Waltham, MA, USA). The X-ray diffraction (XRD) pattern was measured using an X-ray diffractometer (X'Pert-MPD PW 3050) equipped with Cu K α radiation. Inductively coupled plasma mass spectrometry (ICP-MS) was performed using NexION 300D (PerkinElmer, USA). The photothermal experiments were conducted using a NIR laser (808 nm, Changchun New Industries Optoelectronics Technology, China). Bright field and fluorescent images of MDA-MB-231 cells were obtained using an inverted fluorescence microscope (Leica DMI300B, Wetzlar, Germany). The MDA-MB-231 cells were imaged using a confocal laser scanning microscope (CLSM, Zeiss LSM 700, Oberkochen, Germany). The two-photon luminescence spectra were captured using a two-photon fluorescence microscope (TPFM) following the system described by Jun et al.¹⁰. The thermographs were recorded using a Flir i5 compact infrared (IR) thermal imaging camera (Flir Systems Inc., Portland, USA).

In vivo fluorescent imaging experiments were performed using a customized reflection mode fluorescent imaging system (OBLABS, Korea). It consisted of a charge-coupled device (CCD) camera (GS3-U3-28S5M-C; Point Grey Research, USA), a camera lens (AC254-040-A; THORLABS, USA), an emission filter (FF01-520/5-25; SEMROCK, USA), an excitation filter (FF01-494/20-25; SEMROCK, USA), a dichroic mirror (FITC-LP01-Clin-25; SEMROCK, USA), a 490-nm light-emitting diode (LED) (M490L4; THORLABS), and a collimated lens (ACL2520U; THORLABS, USA). All fluorescent images were captured using FlyCapture software (Point Grey Research, USA). Image J software was used to process and analyze the fluorescent images.

Stability of FA-COS-TGA-GNRs-DOX

The stability test of FA-COS-TGA-GNRs-DOX was performed in Dulbecco's Modified Eagle's medium (DMEM) supplemented with 10% fetal bovine serum (FBS) under physiological conditions at pH 7.4 and acidic conditions at pH 5.0 and stirred at ambient temperature for 14 days. The samples were characterized by HRTEM. The stability of FA-COS-TGA-GNRs-DOX at room temperature was observed using a UV-vis spectrophotometer for 14 days in various biological conditions such as PBS, deionized water (DW), and DMEM (without phenol red) with 10% FBS. The stability of FA-COS-TGA-GNRs-DOX in various biological conditions before and after 14 days were further characterized by DLS and ZP.

***In vitro* photothermal conversion efficiency**

1.0 mL of FA-COS-TGA-GNRs-DOX aqueous solutions with various concentrations (40, 50, and 60 $\mu\text{g mL}^{-1}$) was introduced in a single well of a 12-well plate and exposed to the 808 nm laser from the top at various power settings of 0.4 W cm^{-2} , 0.6 W cm^{-2} , 0.8 W cm^{-2} , and 1.0 W cm^{-2} for 300 s. The temperature of the aqueous suspensions was measured using a digital thermometer with the thermocouple immersed into the aqueous solutions¹¹. An IR thermal imaging camera was placed on top of the aqueous solutions, and thermographs were monitored using the IR camera. The thermographs were examined using FLIR software. To determine photothermal stability, 1.0 mL of FA-COS-TGA-GNRs-DOX (60 $\mu\text{g mL}^{-1}$) was exposed to the 808 nm laser at 1.0 W cm^{-2} for 300 s. The procedures of turning on the laser for 300 s and turning off the laser for 900 s were repeated five times. The UV-vis-NIR spectra of FA-COS-TGA-GNRs-DOX were observed after exposure to repeated five cycles of laser irradiation and FA-COS-TGA-GNRs-DOX was also characterized by HRTEM, DLS, and zeta potential after irradiation. The photothermal conversion efficiency of FA-COS-TGA-GNRs-DOX was determined according to previous literatures^{12, 13}.

The FA-COS-TGA-GNRs-DOX ($60 \mu\text{g mL}^{-1}$) aqueous solutions were exposed to the 808 nm laser at 1.0 W cm^{-2} for 300 s, then the laser was turned off, and the temperature decrease of the FA-COS-TGA-GNRs-DOX solution was monitored to measure the rate of heat transfer from the FA-COS-TGA-GNRs-DOX aqueous solution system to the environment. The photothermal conversion efficiency (η value) was calculated using the following equation:

$$\eta = \frac{hS(T_{Max} - T_{Sur}) - Q_{dis}}{I(1 - 10^{-A_{808}})}$$

Cell culture

MDA-MB-231 cells and MCF-7 cells (human breast cancer cell line) were purchased from ATCC. Cells were plated and cultured in DMEM (Hyclone) supplemented with 10% FBS (Hyclone) and 1% penicillin-streptomycin (Hyclone) at $37 \text{ }^\circ\text{C}$ under 5% CO_2 conditions.

***In vitro* biocompatibility test**

In vitro biocompatibility evaluation of FA-COS-TGA-GNRs was performed using MDA-MB-231 cells and MCF-7 cells. The cells (50,000 cells per well) were cultured in 96 multiwell plates for 24 h and 48 h. Afterward, cells were treated with various concentrations of FA-COS-TGA-GNRs (5, 15, 25, 75, 100, 150, and $200 \mu\text{g mL}^{-1}$) for 24 h and 48 h. Then, 3-(4,5-dimethylthiazol-2-yl)-2,5-diphenyltetrazolium bromide (MTT) solution was added into all of the wells and the absorbance of each well at 570 nm was measured using a microplate reader (TECAN Infinite F50).

***In vitro* hemocompatibility test**

To assess *in vitro* hemocompatibility, mice blood was successfully collected by cardiac puncture, and blood samples were stabilized using ethylenediaminetetraacetic acid (EDTA). 1 mL of blood sample was added into 2 mL PBS, and the red blood cells (RBCs) were collected by centrifugation

at 1500 rpm for 15 min and were diluted into 10 mL pre-chilled PBS. 0.2 mL of RBC was incubated with 0.8 mL FA-COS-TGA-GNRs dispersions at various concentrations (10, 25, 50, 100, 150, and 200 $\mu\text{g mL}^{-1}$) and was also treated with PBS (negative control) and deionized water (positive control). All samples were treated at 37 °C for 4 h and centrifuged at 15000 rpm for 3 min. The absorbance of each sample at 541 nm was observed using a UV–vis spectrophotometer. The hemolytic percentage was calculated using the following equation: ¹⁴

$$\text{Hemolysis percent (\%)} = \frac{A_{\text{sample}} - A_{\text{negative}}}{A_{\text{positive}} - A_{\text{negative}}} \times 100\%$$

***In vitro* cytotoxicity**

The cell viability of MDA-MB-231 cells was assessed using an MTT assay. MDA-MB-231 cells (50,000 cells per well) were cultured in 96 multiwell plates for 24 h. Afterward, cells were incubated with various concentrations of FA-COS-TGA-GNRs-DOX (5, 10, 25, 50, 75, 100, and 200 $\mu\text{g mL}^{-1}$) for 24 h and 48 h. Then, the MTT solution was added into each well, and the optical densities of all of the wells were measured at 570 nm using a microplate reader.

Cellular uptake

MDA-MB-231 (1×10^5 cells per well) cells were plated in 12 multiwell plates and incubated at 37 °C for 24 h. The cells were incubated with 0.5 mg mL^{-1} free FA to occupy the FA receptor of the cells and were incubated with COS-TGA-GNRs-DOX and FA-COS-TGA-GNRs-DOX (5 $\mu\text{g mL}^{-1}$ of DOX) for an additional 3 h. After that, the cells were washed three times with PBS, and then, the cells were trypsinized and suspended in PBS. The intensity of DOX fluorescence was evaluated using a flow cytometer (BD FACSVerser, NJ, USA).

To quantify the amount of FA-COS-TGA-GNRs-DOX uptake in MDA-MB-231 cells, cells (1×10^5 cells per well) were cultured in six multiwell plates and incubated for 24 h. The cells were treated with 60 $\mu\text{g mL}^{-1}$ COS-TGA-GNRs-DOX or FA-COS-TGA-GNRs-DOX and

collected at 1, 2, 4, 6, 8, 12, 18, and 24 h by centrifugation. At each time point, the cells were washed three times in PBS for three times, counted using a hemocytometer, and digested with aqua regia. The gold (Au) concentrations were quantified by ICP-MS and Au content was expressed in picogram of Au per cell.¹⁵

***In vitro* photothermal therapy**

MDA-MB-231 (50,000 cells per well) cells were cultured in 96 multiwell plates for 24 h prior to assay. Then the cells were incubated with different concentrations of free DOX, FA-COS-TGA-GNRs, and FA-COS-TGA-GNRs-DOX (10, 20, 30, 40, 50 and 60 $\mu\text{g mL}^{-1}$) for 6 h. The cells were or were not exposed to the 808 nm laser (1.0 W cm^{-2}) for 300 s. The cells were treated at 37 °C for another 3 h, and then, cell viability was assessed using the MTT assay. In addition, cells were treated with 60 $\mu\text{g mL}^{-1}$ FA-COS-TGA-GNRs-DOX for 6 h, and then, the cells were or were not exposed to the 808 nm laser at various power settings of 0.4 W cm^{-2} , 0.6 W cm^{-2} , 0.8 W cm^{-2} , and 1.0 W cm^{-2} for 300 s. After incubation for an additional 3 h, cell viability was assessed using the MTT assay.

***In vitro* cell imaging**

MDA-MB-231 (1×10^5 cells per well) cells were cultured in six multiwell plates at 37 °C for 24 h. Afterward, the cells were divided into six groups: group 1, with cells only; group 2, with laser irradiation (1.0 W cm^{-2}) only; group 3, incubation with free DOX (60 $\mu\text{g mL}^{-1}$); group 4, incubation with FA-COS-TGA-GNRs (60 $\mu\text{g mL}^{-1}$) only; group 5, incubation with FA-COS-TGA-GNRs-DOX (60 $\mu\text{g mL}^{-1}$) only; and group 6, incubation with FA-COS-TGA-GNRs-DOX (60 $\mu\text{g mL}^{-1}$) with laser irradiation at 1.0 W cm^{-2} for 300 s. After treatment, all groups of cells were incubated for another 3 h, and all of the cells were stained with calcein-AM and propidium iodide (PI) for visualization of live (green) and dead (red) cells, respectively. Then, the cells were washed twice

with PBS, and the images of the five samples were examined under an inverted fluorescence microscope.

MDA-MB-231 (1×10^5 cells per well) cells were cultured onto glass coverslips in six multiwell plates and incubated at 37 °C for 24 h. The cells were incubated with 60 $\mu\text{g mL}^{-1}$ FA-COS-TGA-GNRs-DOX for an additional 6 h. Afterward, the cells were exposed to the 808 nm laser (1.0 W cm^{-2}) for 300 s. Then, the cells were incubated at 37 °C for 1, 2, and 3 h and the cell nuclei were stained with Hoechst 33342 for 30 min. The cells were washed three times with PBS and were captured under a CLSM.

***In vitro* two-photon fluorescence imaging**

MDA-MB-231 (1×10^5 cells per well) cells were incubated onto glass coverslips in six multiwell plates at 37 °C for 24 h. All groups of cells were further incubated with saline, free DOX, FA-COS-TGA-GNRs, and FA-COS-TGA-GNRs-DOX for 6 h, and the cells were or were not exposed to the 808 nm laser at 1.0 W cm^{-2} for 300 s. All groups of cells were cultured at 37 °C for 3 h, and the cell nuclei were stained with Hoechst 33342 for 30 min. Finally, all of the cells were washed three times with PBS and were captured using a two-photon fluorescent microscope (TPFM).

Apoptosis assay

The MDA-MB-231 cells (3×10^5 cells per well) were cultured in 12 multiwell plates at 37 °C for 24 h. The cells were incubated with saline, free DOX, FA-COS-TGA-GNRs, and FA-COS-TGA-GNRs-DOX for 6 h. Then, all of the cells were or were not exposed to the 808 nm laser at 1.0 W cm^{-2} for 300 s, and the cells were incubated at 37 °C for another 3 h. Finally, all groups of cells were harvested, washed three times in PBS, and stained with an Annexin V-FITC/PI apoptosis detection kit, and then, all groups of cells were analyzed using flow cytometry (BD FACSVerser, BD Biosciences, NJ, USA).

***In vitro* fluorescence cellular imaging**

The conjugation of fluorescein isothiocyanate (FITC) with the free amino groups of COS was prepared according to earlier work ^{16, 17}. The MDA-MB-231 (2×10^5 cells per well) cells were cultured in 24 multiwell plates at 37 °C for 24 h. The cells were incubated with FITC-labelled FA-COS-TGA-GNRs-DOX ($60 \mu\text{g mL}^{-1}$) for 6 h and then were exposed to the 808 nm laser (1.0 W cm^{-2}) for 300 s and incubated for another 3 h. After washing, the fluorescence images of cells at different time periods (2, 4, 6, and 8 h) were captured using a customized reflection mode fluorescent imaging system.

***In vitro* photoacoustic imaging**

The photoacoustic tomography (PAT, OBLABS, Korea) system was described in our previous work ^{18, 19}. A polyvinyl alcohol (PVA) phantom that closely mimics human tissues was developed according to the previous work ¹⁹. MDA-MB-231 (1×10^5 cells per well) cells were incubated with different concentrations of FA-COS-TGA-GNRs-DOX (40, 50 and $60 \mu\text{g mL}^{-1}$) at 37 °C for 6 h. After incubation, the cells were harvested, and the PAI of the cell pellets were mixed with 10% gelatin and were added into all of the wells in the tissue-mimicking PVA phantom.

Statistical analysis

Quantified data were presented as the mean \pm SD. Statistical significance was assessed using the *t*-test. Statistical significance was set at $*P < 0.05$ and $**P < 0.01$. Origin 8.0 software was used to analyze the data.

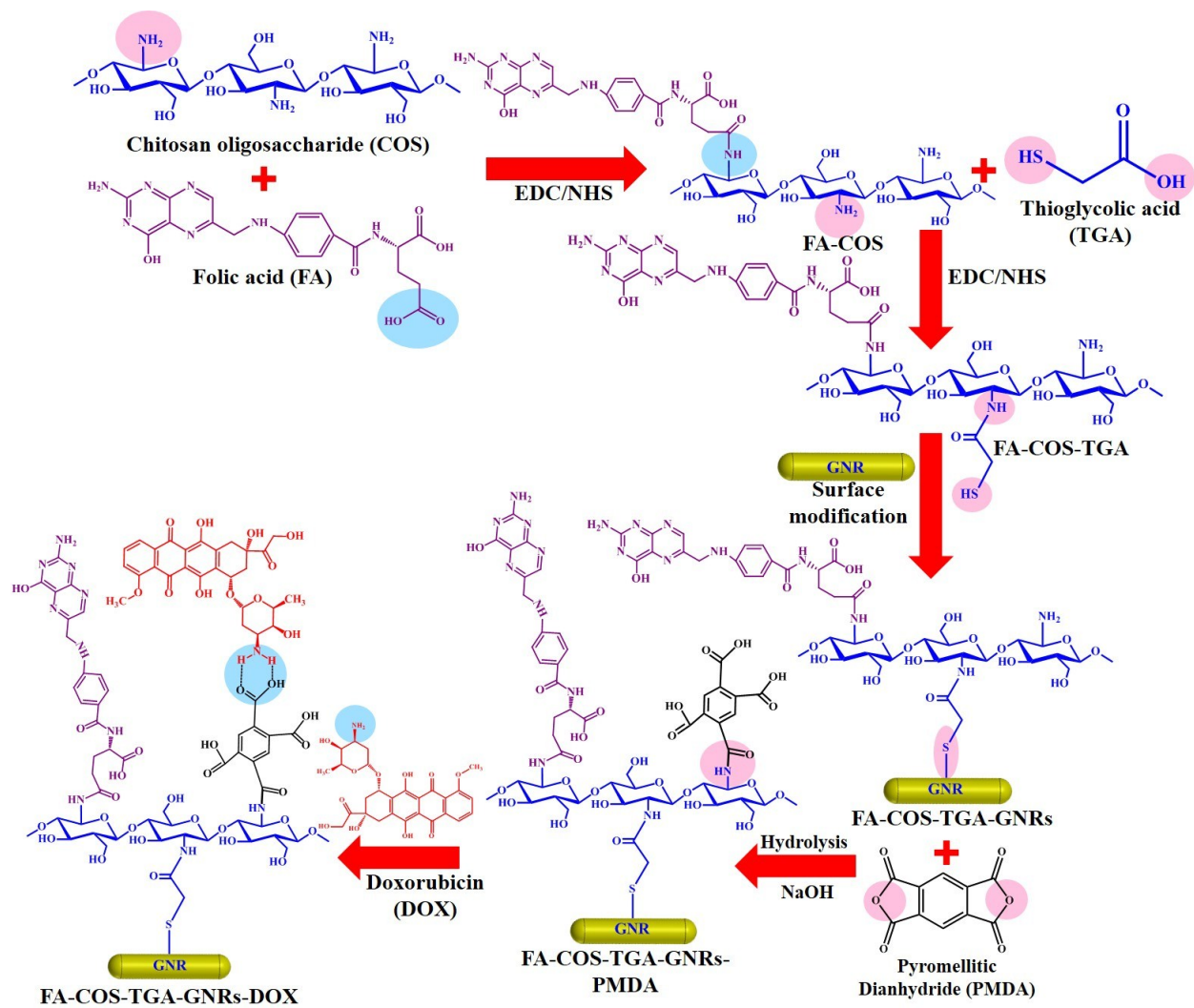


Fig. S1. Synthetic route of FA-COS-TGA-GNRs-DOX.

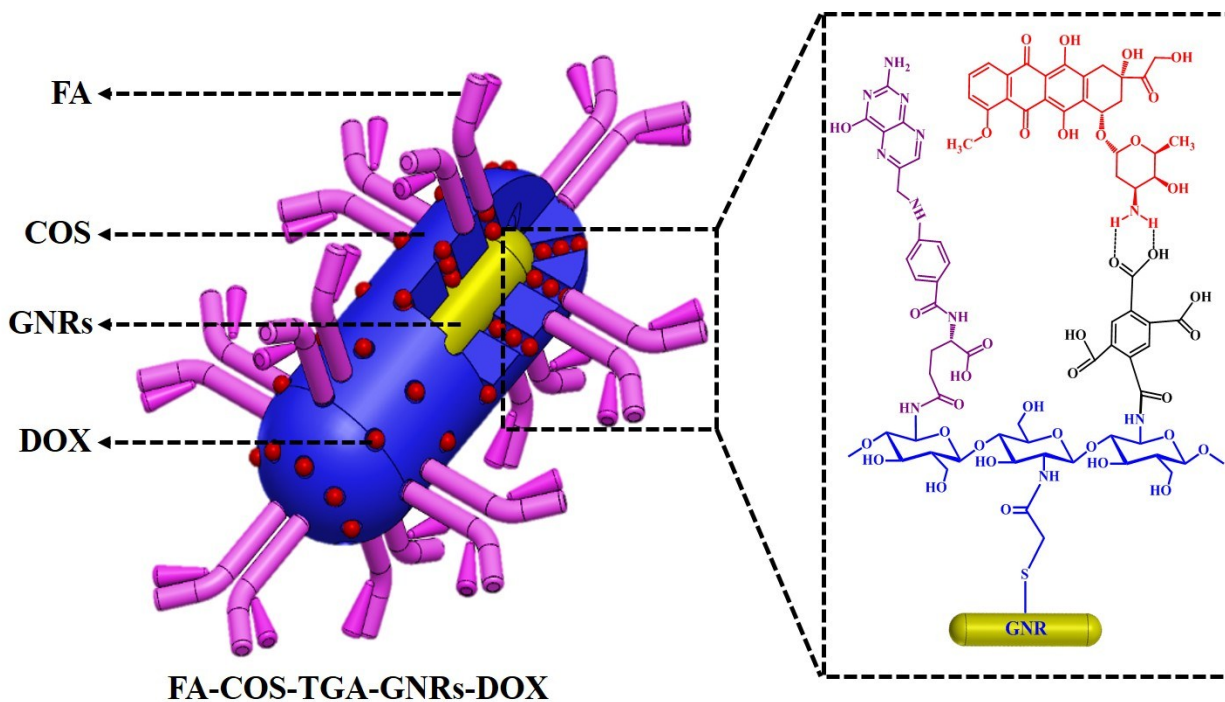


Fig. S2. Schematic of the preparation of FA-COS-TGA-GNRs-DOX.

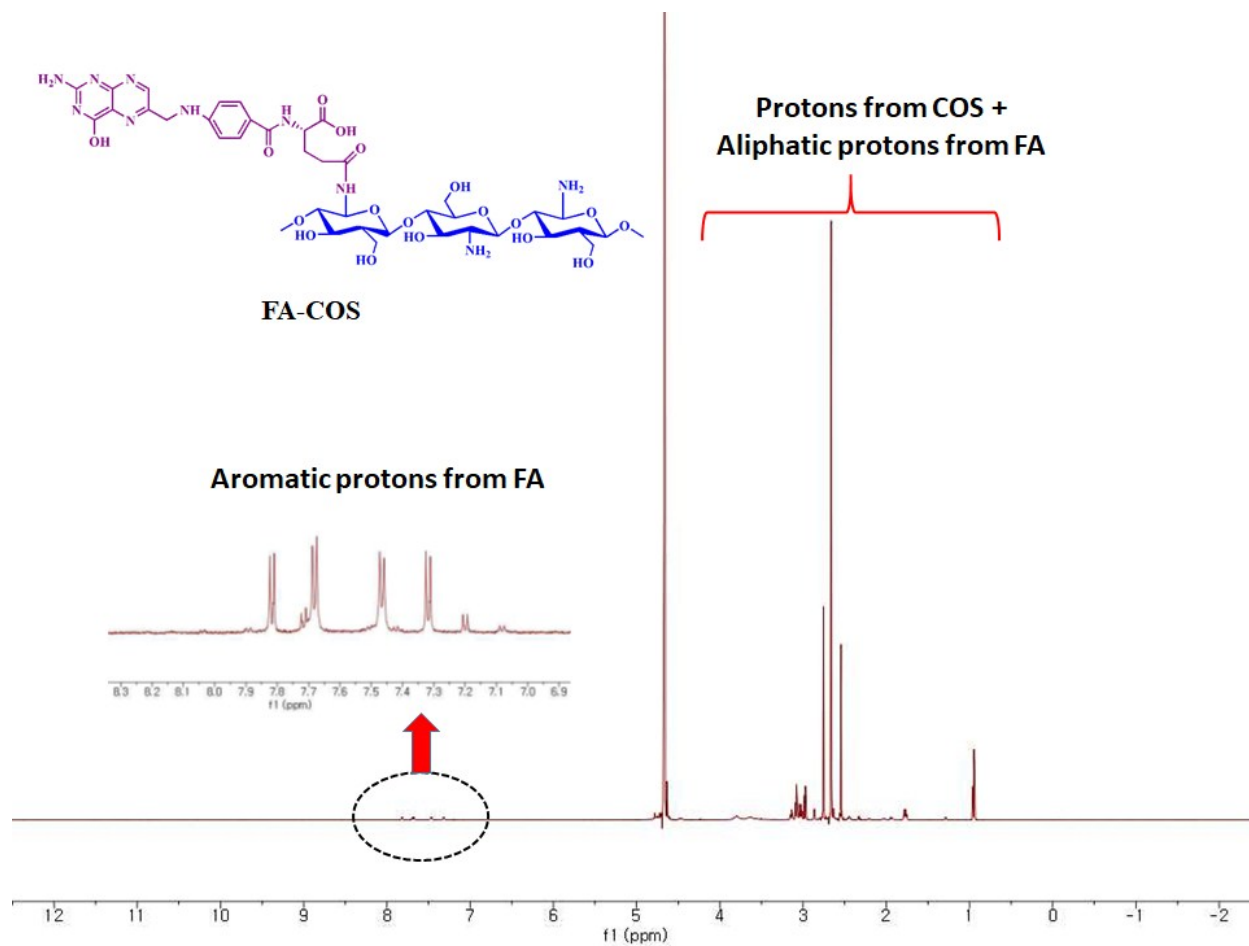


Fig. S3. ¹H NMR spectra of FA-COS at 25 °C.

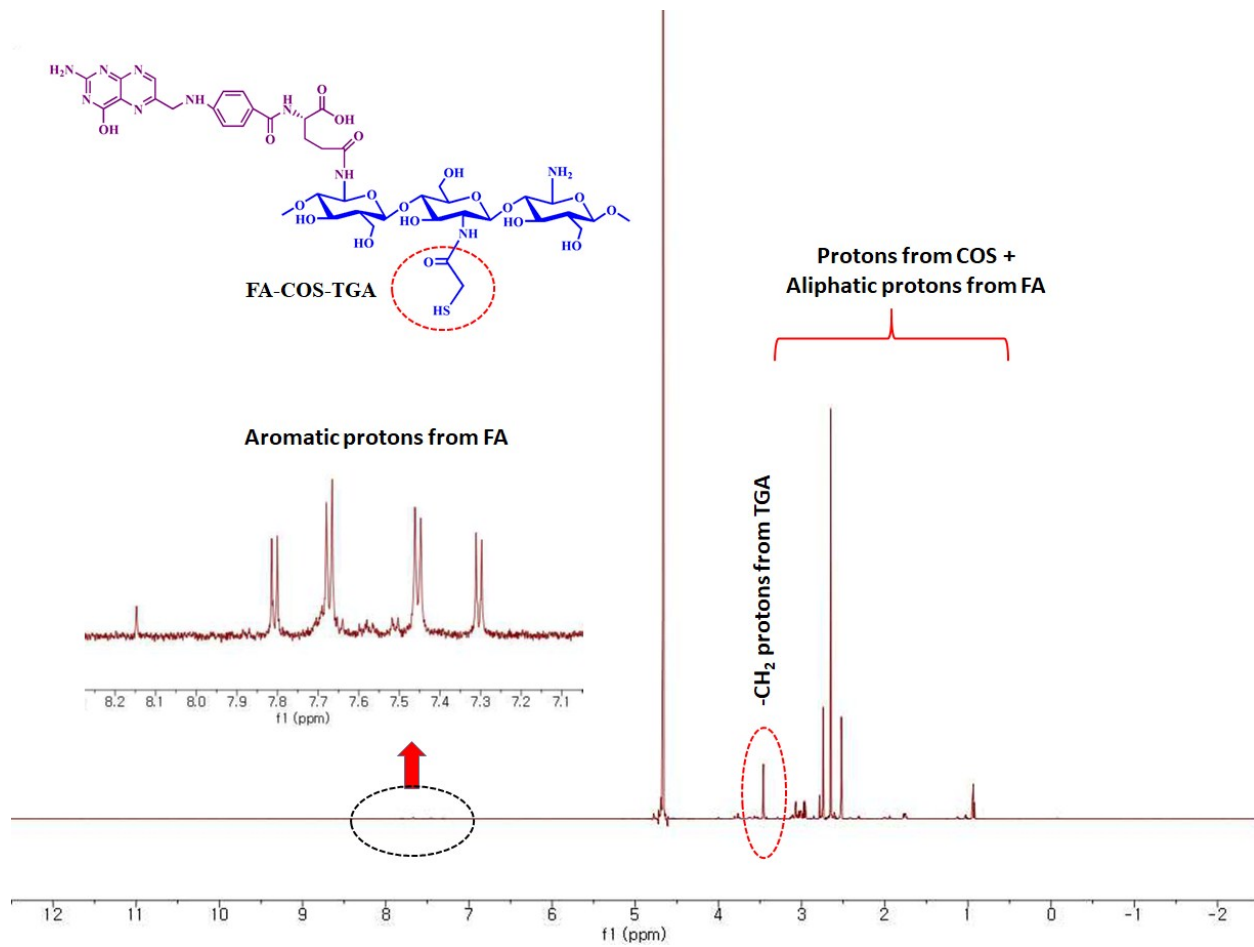


Fig. S4. ¹H NMR spectra of FA-COS-TGA at 25 °C.

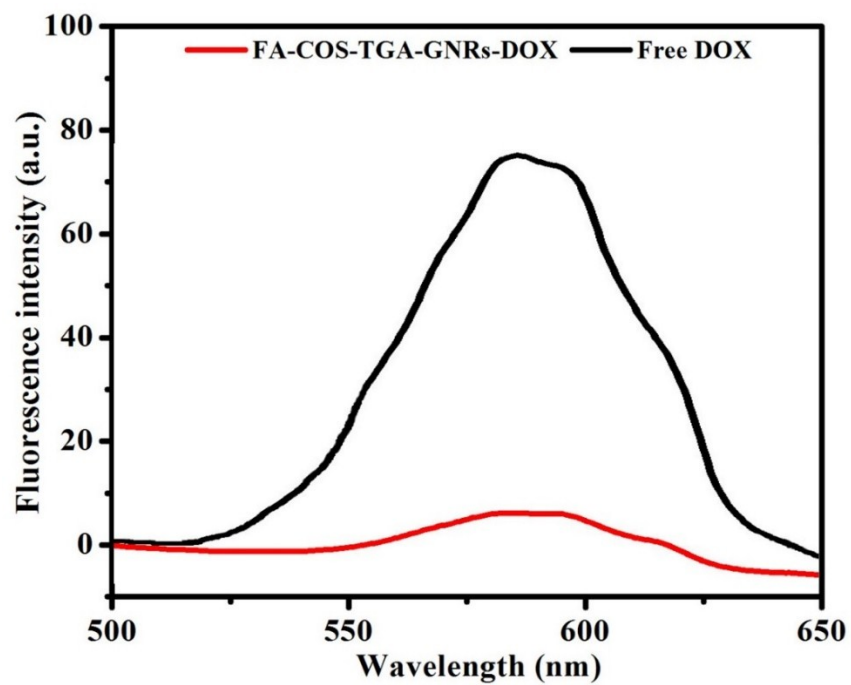


Fig. S5. Fluorescence spectra of free DOX and FA-COS-TGA-GNRs-DOX with the same concentration of DOX. Significant fluorescence quenching was observed for FA-COS-TGA-GNRs-DOX.

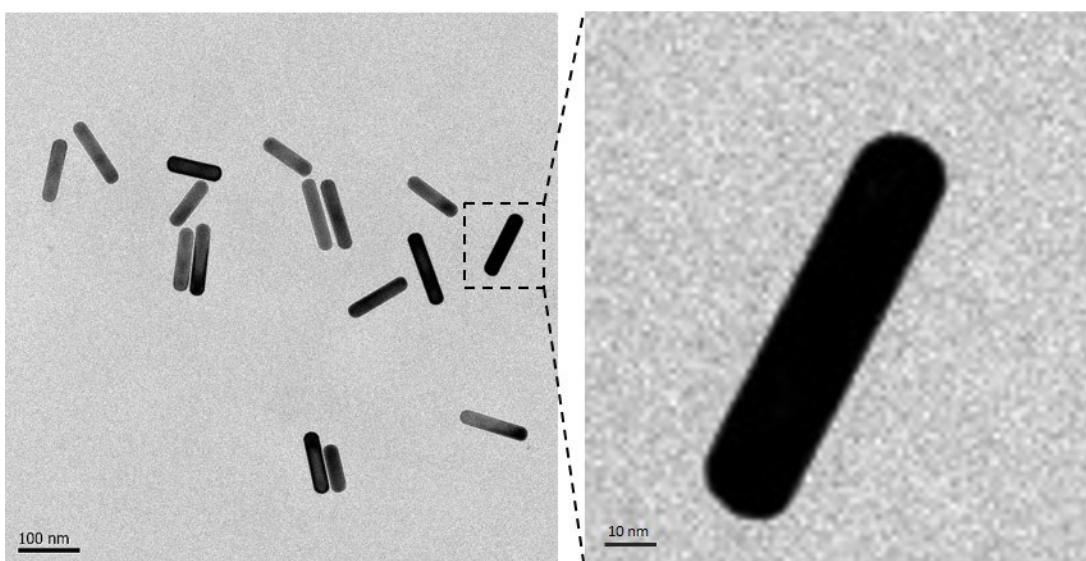


Fig. S6. HRTEM images of GNRs.

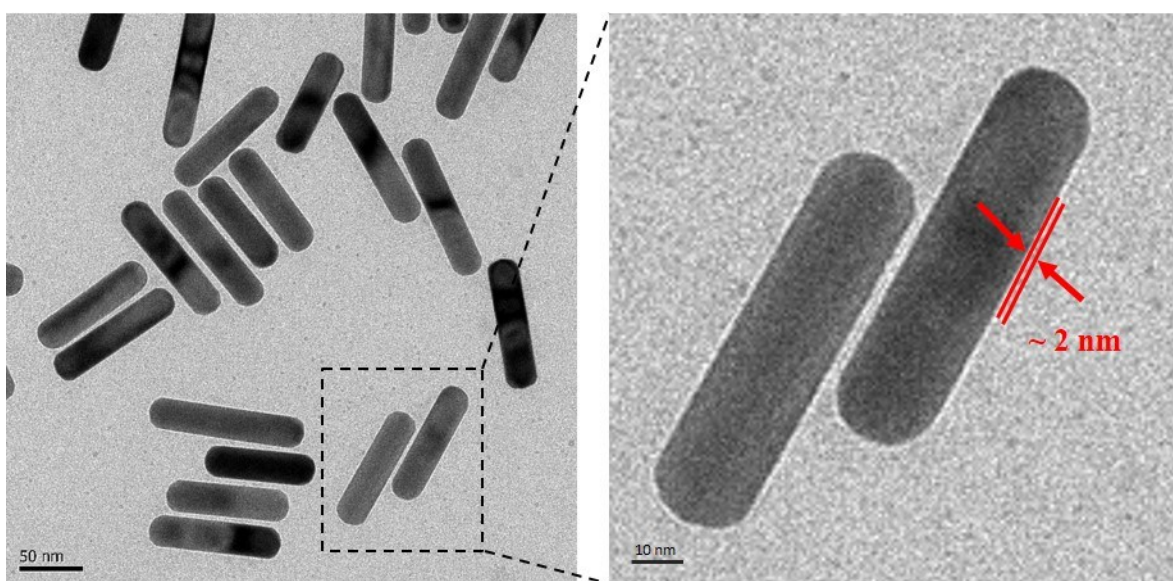


Fig. S7. HRTEM images of FA-COS-TGA-GNRs.

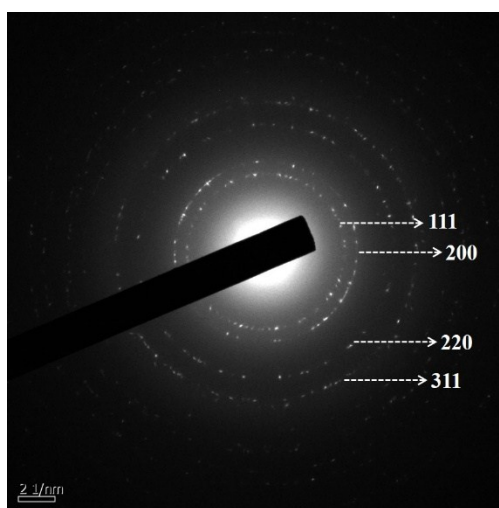


Fig. S8. Selected area electron diffraction (SAED) pattern of FA-COS-TGA-GNRs-DOX

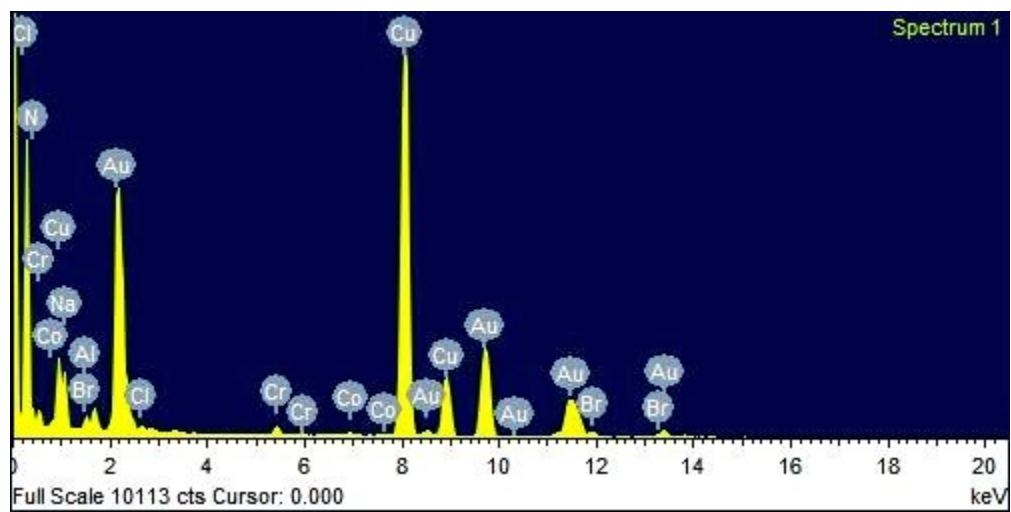


Fig. S9. Energy dispersive X-ray spectroscopy (EDX) of FA-COS-TGA-GNRs-DOX

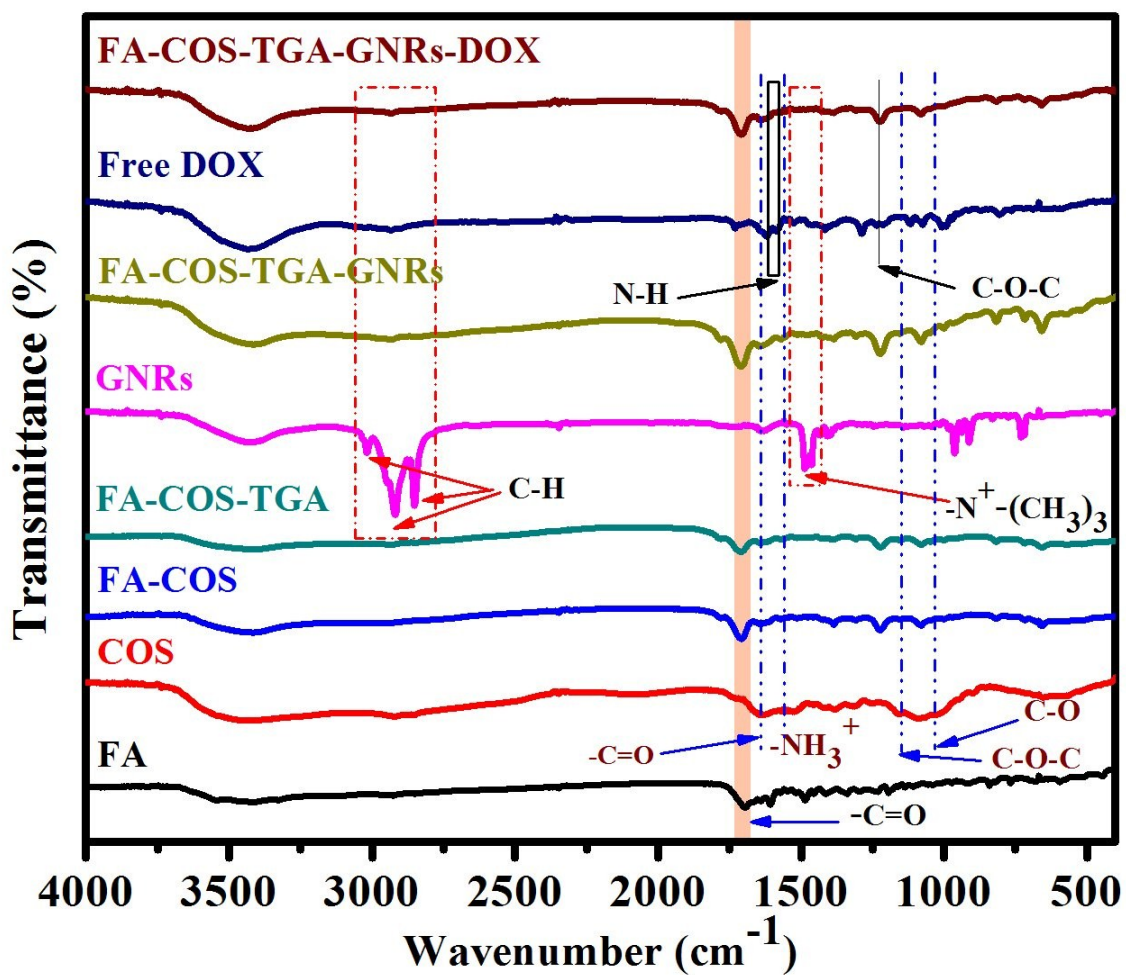


Fig. S10. FTIR spectra of FA, COS, FA-COS, FA-COS-TGA, GNRs, FA-COS-TGA-GNRs, free DOX, and FA-COS-TGA-GNRs-DOX.

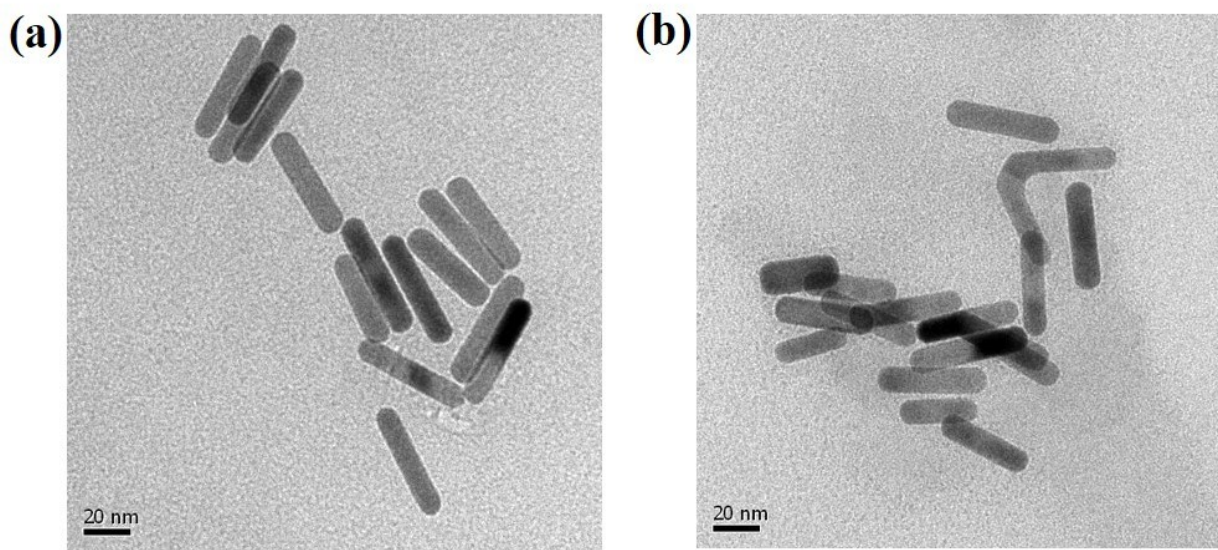


Fig. S11. HRTEM images of FA-COS-TGA-GNRs-DOX in DMEM with 10% FBS under both neutral at pH 7.4 and acidic conditions at pH 5.0.

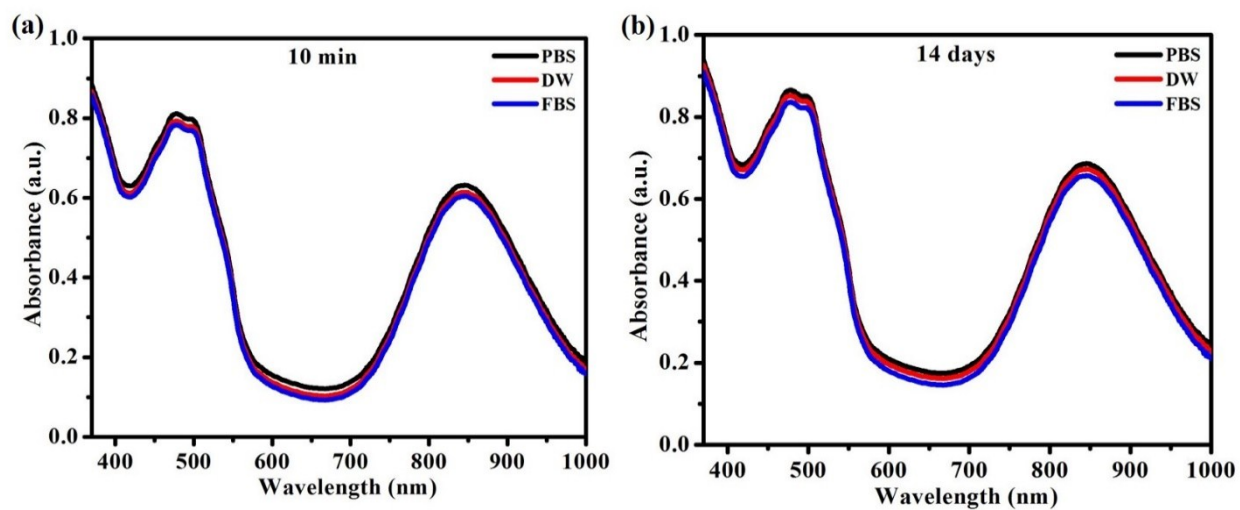


Fig. S12. UV-vis spectra of FA-COS-TGA-GNRs-DOX in various biological conditions before and after 14 days.

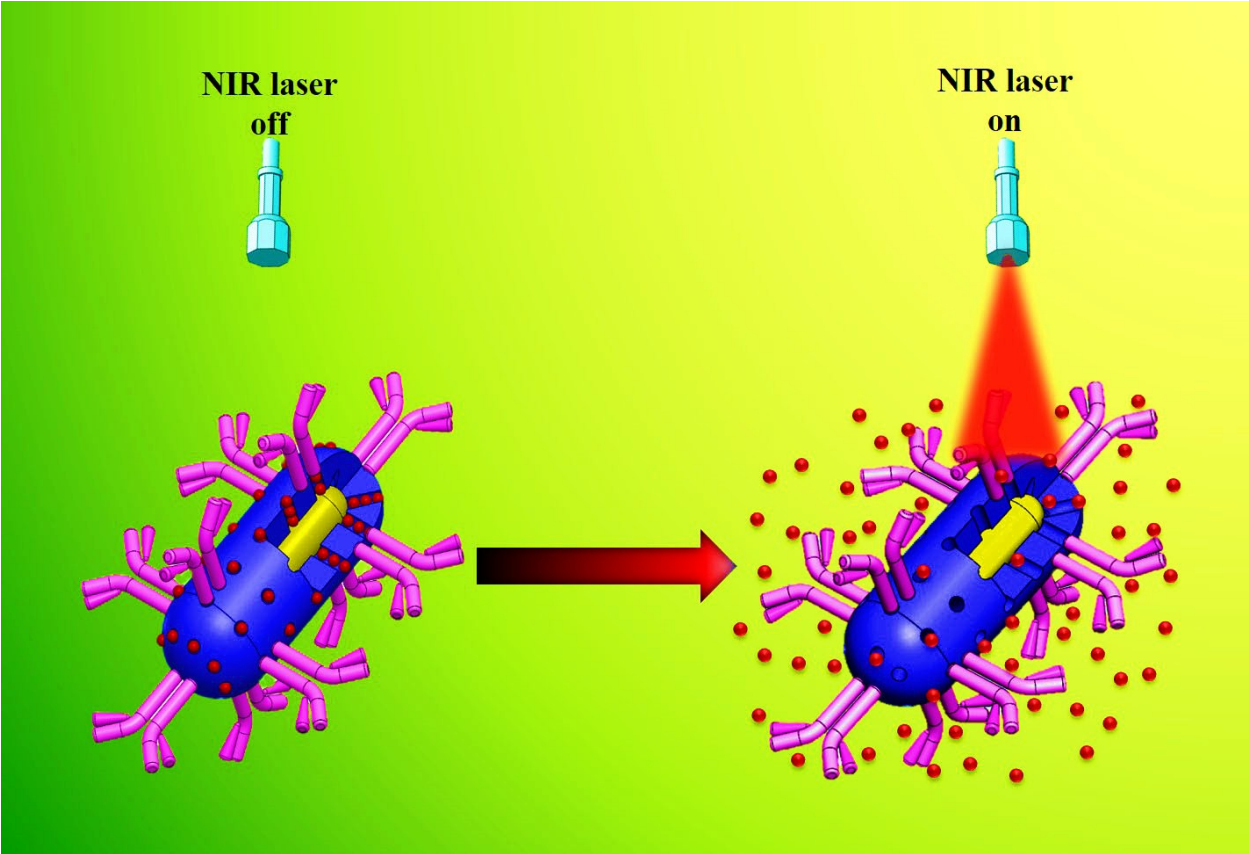


Fig. S13. Schematic diagram of DOX release from FA-COS-TGA-GNRs-DOX with laser irradiation.

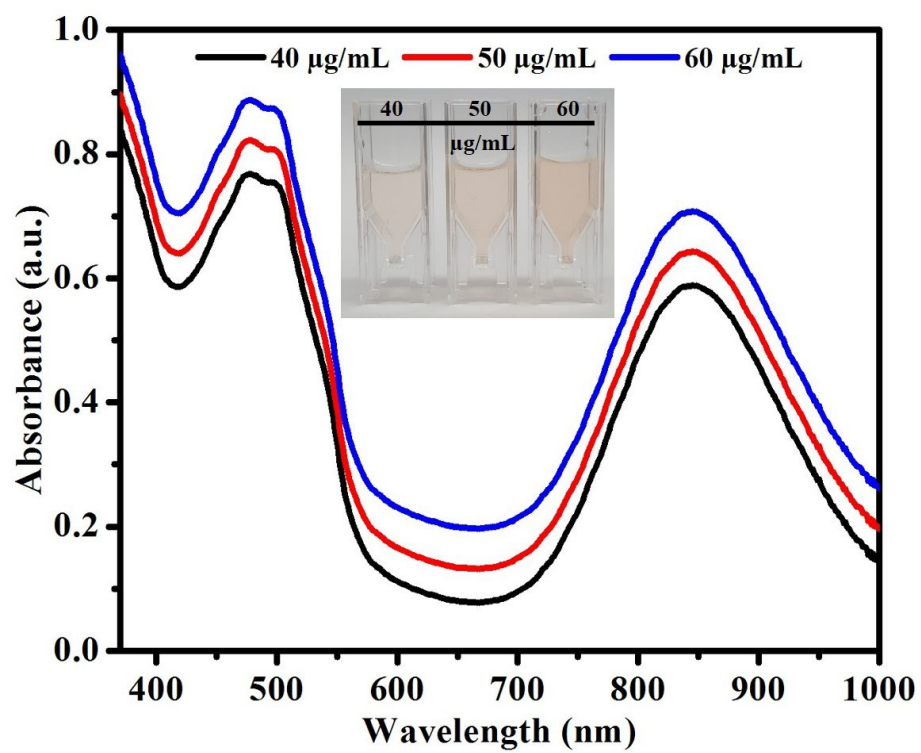


Fig. S14. UV-vis spectra of FA-COS-TGA-GNRs-DOX in various concentrations and inset image showed the FA-COS-TGA-GNRs-DOX aqueous solutions in various concentrations.

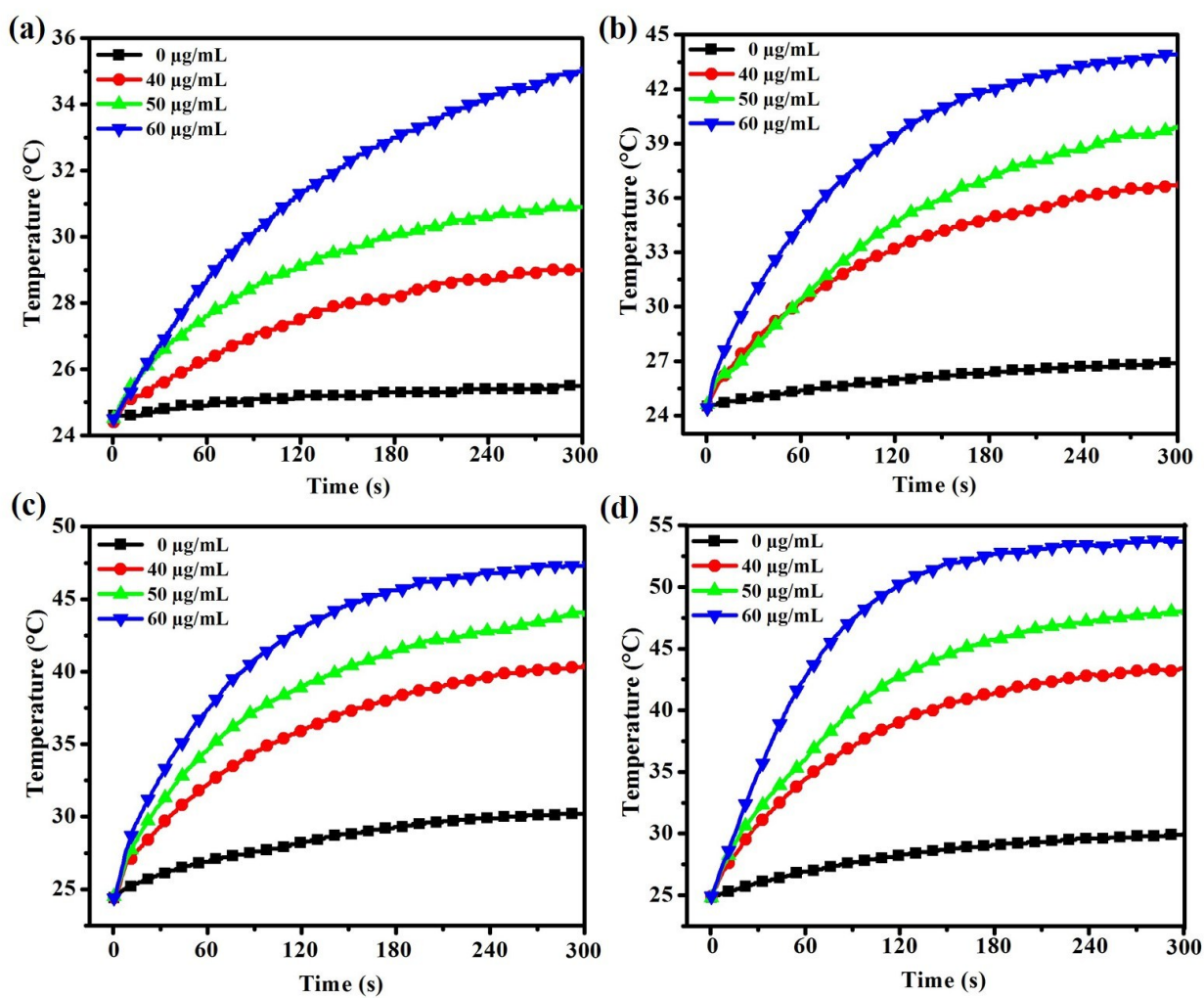


Fig. S15. Temperature elevation of FA-COS-TGA-GNRs-DOX aqueous solution at various concentrations under 808 nm laser irradiation at various power settings of $0.4\ W\ cm^{-2}$ (a), $0.6\ W\ cm^{-2}$ (b), $0.8\ W\ cm^{-2}$ (c), and $1.0\ W\ cm^{-2}$ (d) for 300 s.

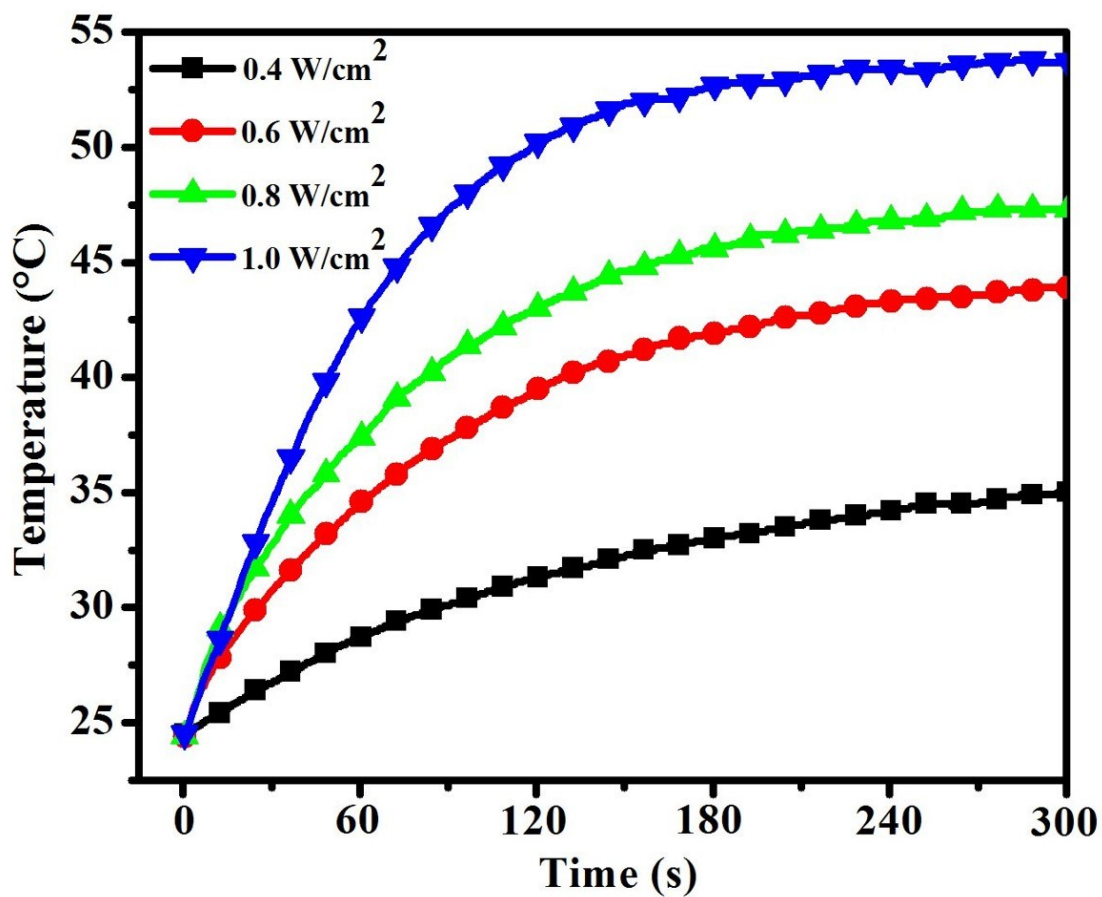


Fig. S16. Temperature elevation of FA-COS-TGA-GNRs-DOX aqueous solution at concentration of $60 \mu\text{g mL}^{-1}$ under 808 nm laser irradiation at various power settings of 0.4 W cm^{-2} , 0.6 W cm^{-2} , 0.8 W cm^{-2} , and 1.0 W cm^{-2} for 300 s.

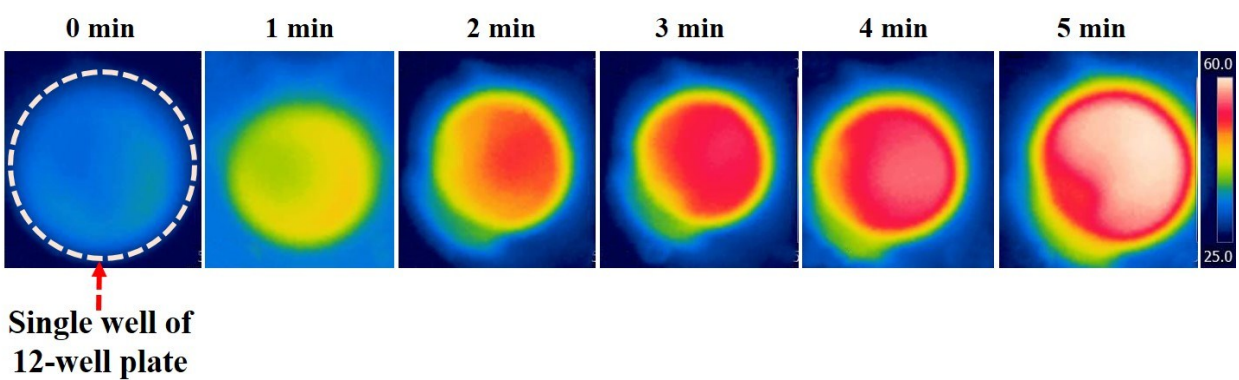


Fig. S17. IR thermal image of the FA-COS-TGA-GNRs-DOX ($60 \mu\text{g mL}^{-1}$) aqueous solution in a single well of a 12-well plate under 808 nm laser irradiation at 1.0 W cm^{-2} for different times.

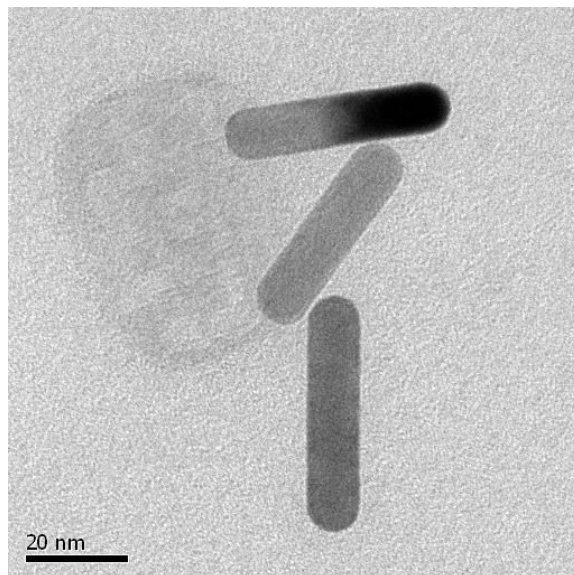


Fig. S18. HRTEM images of FA-COS-TGA-GNRs-DOX after five cycles of the laser on/off.

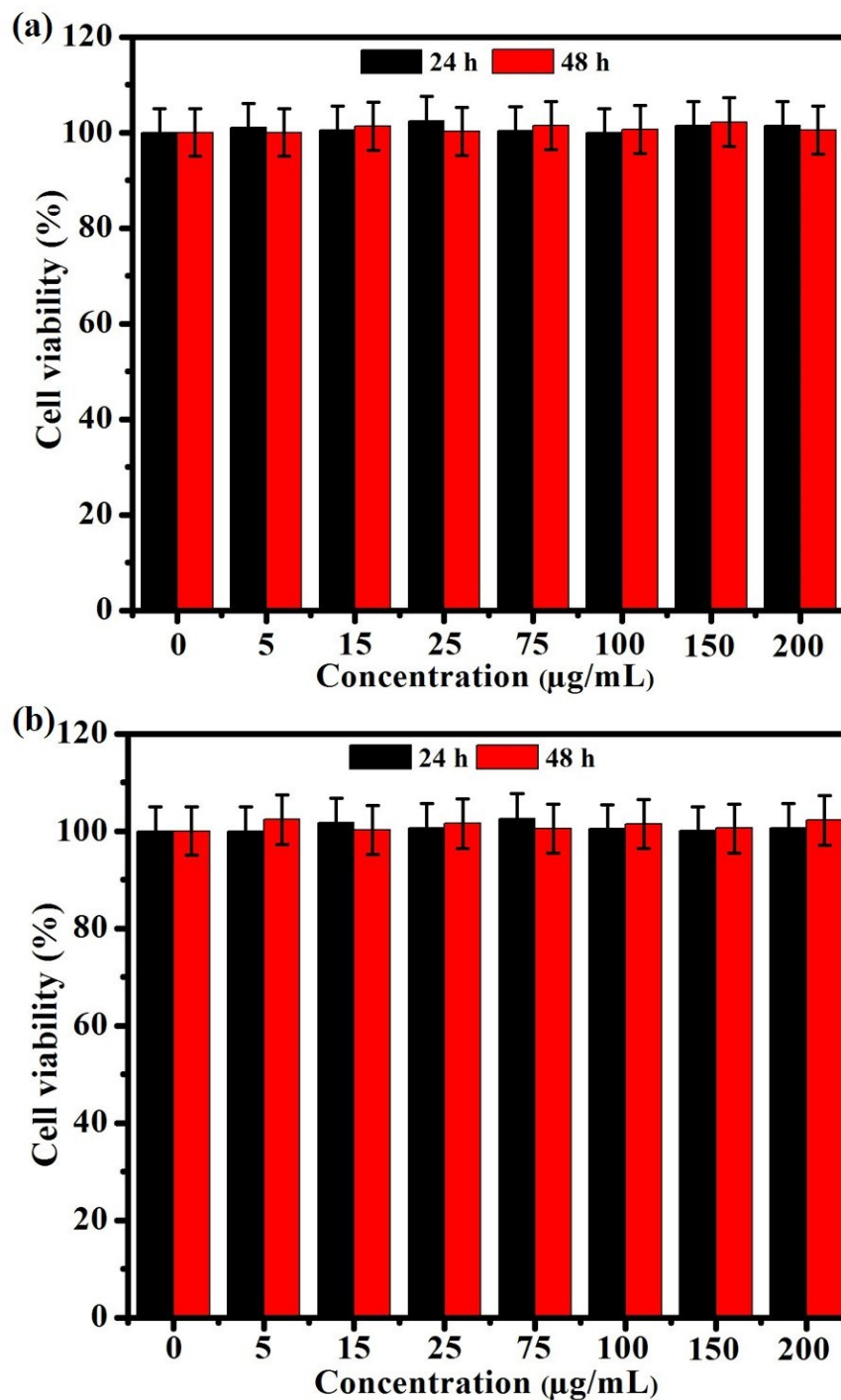


Fig. S19. Cell viabilities of MDA-MB-231 cells (a) and MCF-7 cells (b) treated with FA-COS-TGA-GNRs with various concentrations for 24 and 48 h. Data are represented as mean \pm standard derivation (SD) for the three experiments.

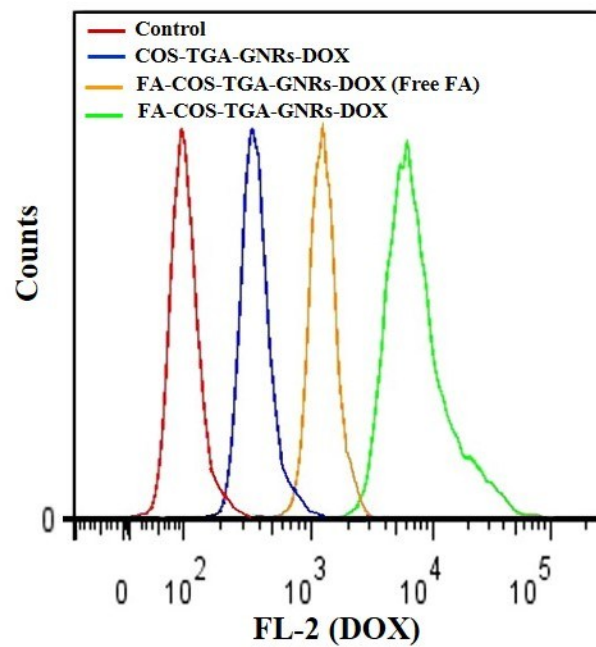


Fig. 31

Fig. S20. Quantitative uptake of analysis by flow cytometry of COS-TGA-GNRs-DOX, FA-COS-TGA-GNRs-DOX pretreated with FA, and FA-COS-TGA-GNRs-DOX on MDA-MB-231 cells.

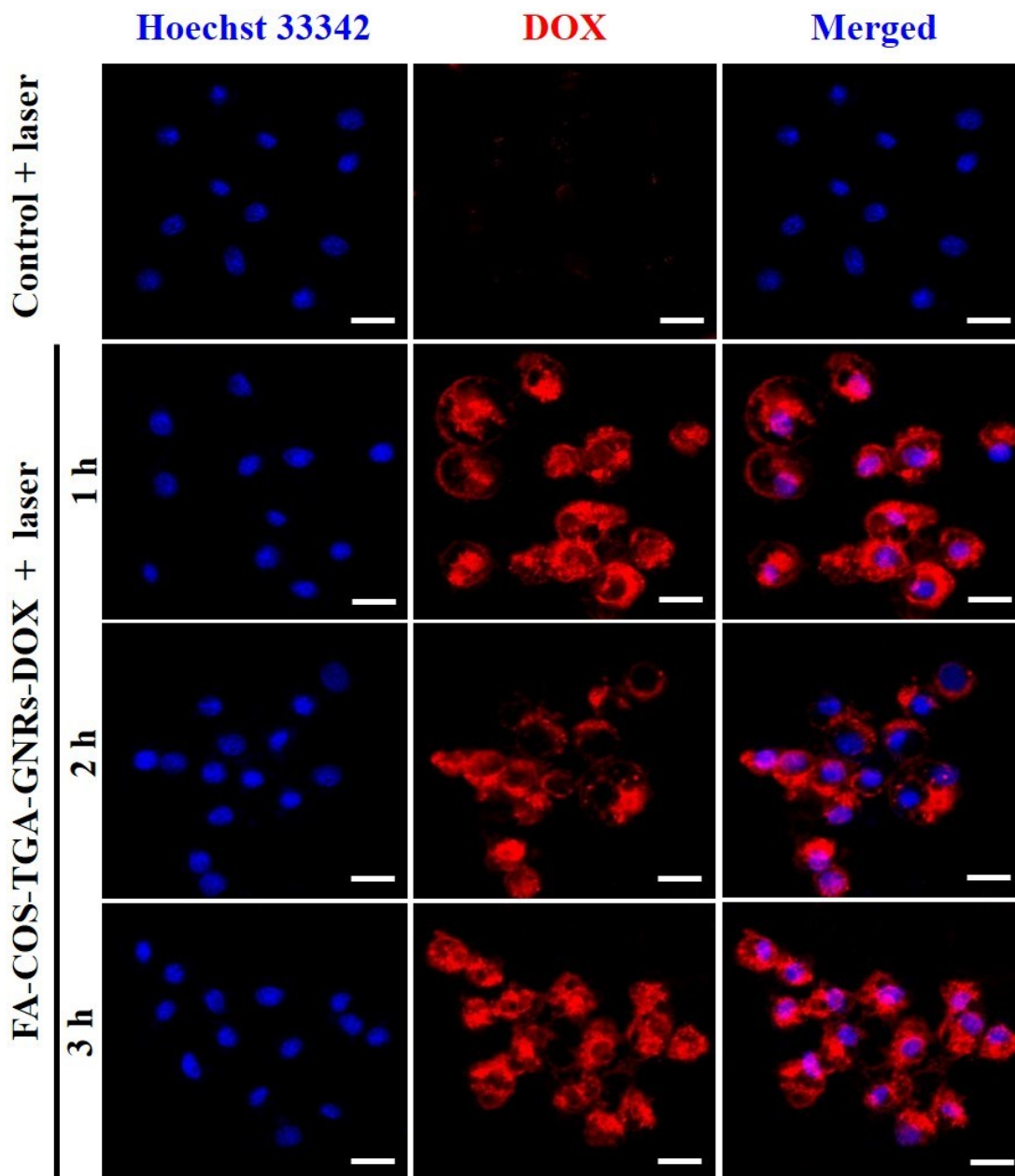


Fig. S21. CLSM image of MDA-MB-231 cells treated with or without FA-COS-TGA-GNRs-DOX ($60 \mu\text{g mL}^{-1}$) for 6 h, the cells were exposed to 808 nm laser irradiation at 1.0 W cm^{-2} for 300 s and incubated for another 1 h, 2 h, and 3 h, respectively. Hoechst 33342 for nuclei staining (blue) and released DOX fluorescence (red) were observed. Scale bar: 20 μm .

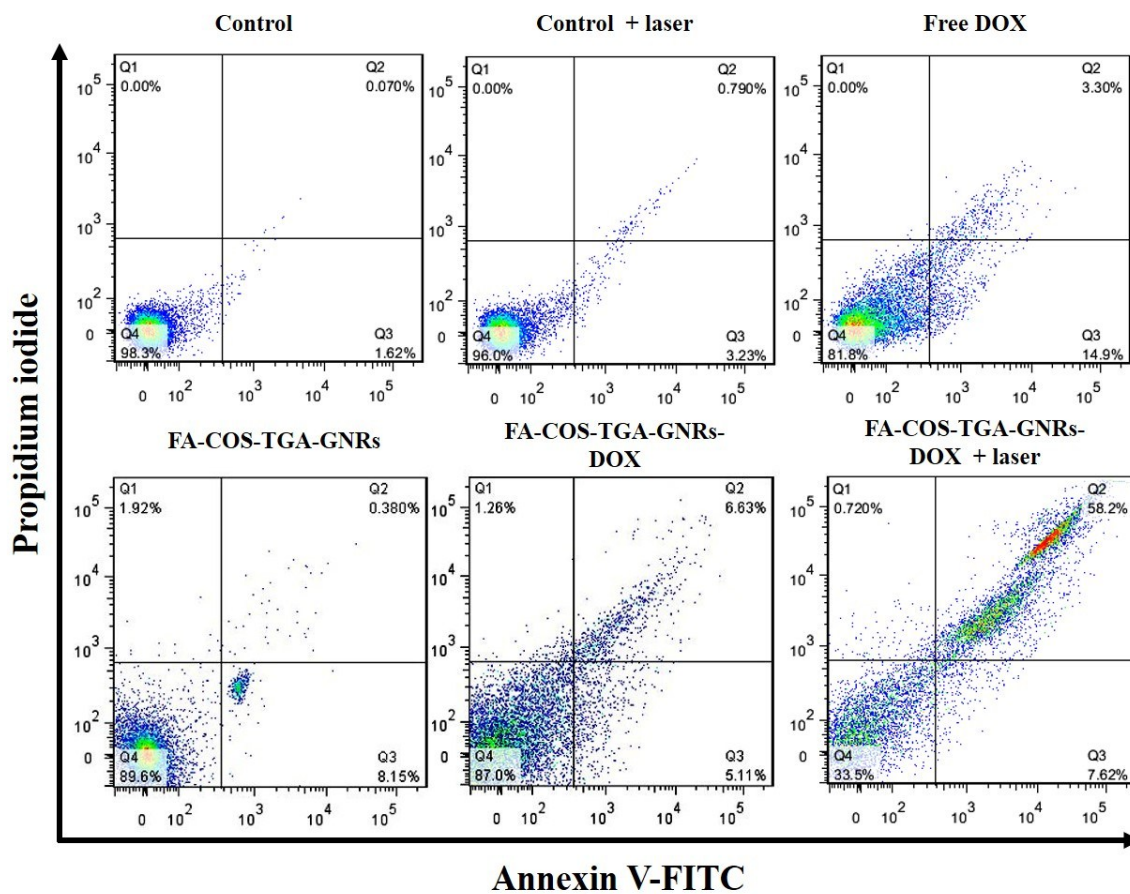


Fig. S22. Flow cytometric analysis of MDA-MB-231 cells death induced by various groups.

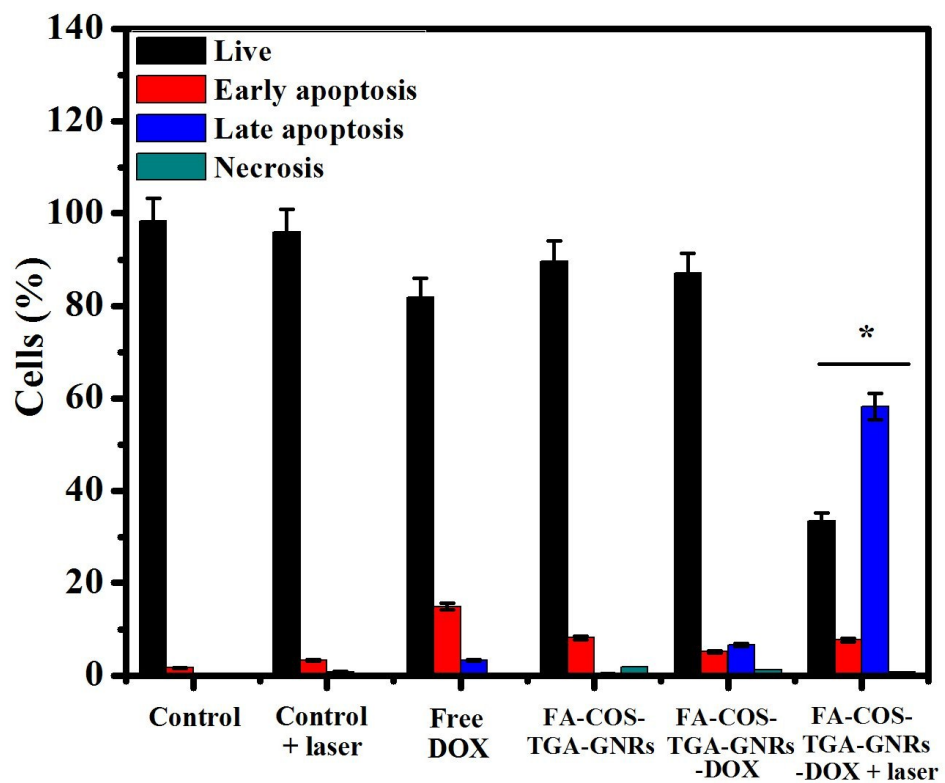


Fig. S23. Quantified analysis of apoptosis/necrosis cells percentage according to double staining by Annexin V and PI. Data are represented as mean \pm standard derivation (SD) for the three experiments (* significant $p < 0.05$).

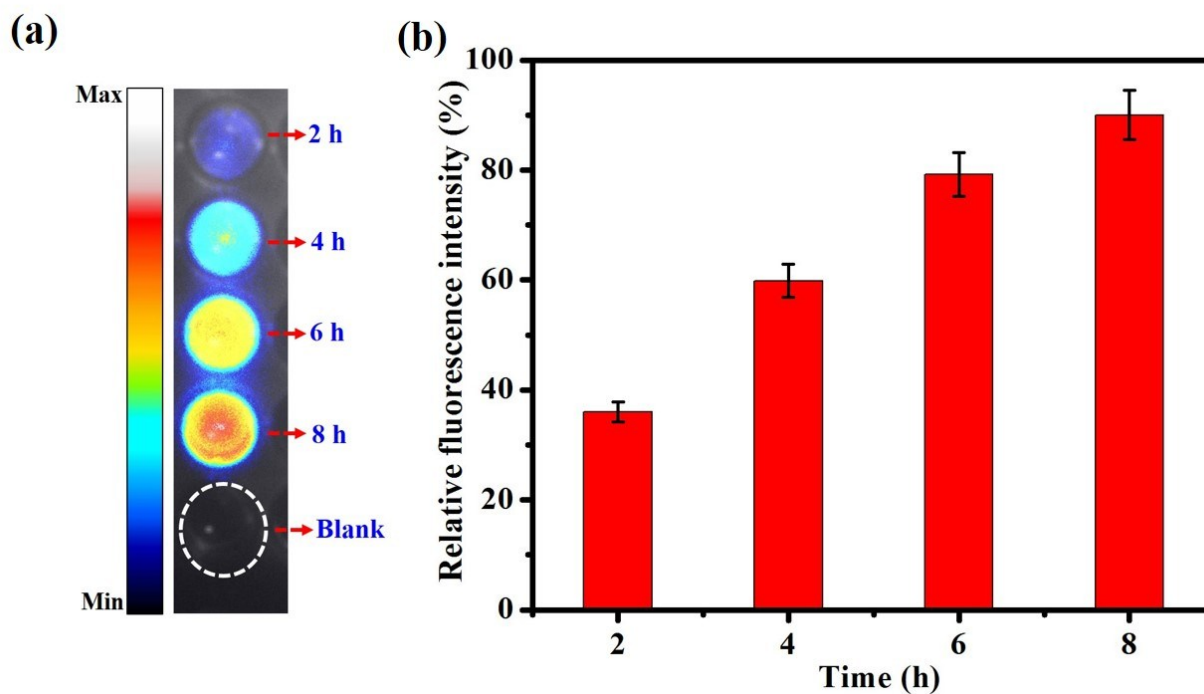


Fig. S24. (a) *In vitro* fluorescence cellular images of MDA-MB-231 cells treated with FITC-labelled FA-COS-TGA-GNRs-DOX ($60 \mu\text{g mL}^{-1}$) at various time points. (b) The fluorescence intensity of MDA-MB-231 cells treated with FITC-labelled FA-COS-TGA-GNRs-DOX ($60 \mu\text{g mL}^{-1}$) at various time points.

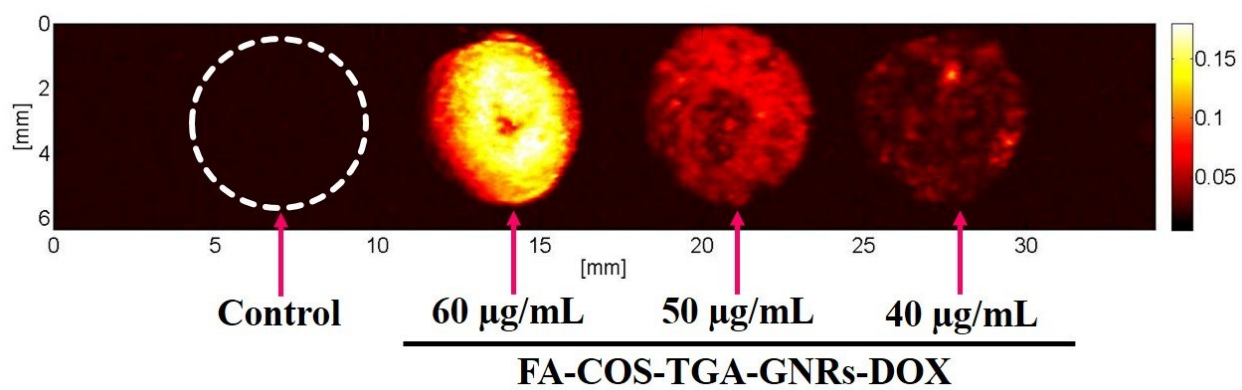


Fig. S25. *In vitro* photoacoustic image of MDA-MB-231 cells treated with various concentration of FA-COS-TGA-GNRs-DOX.

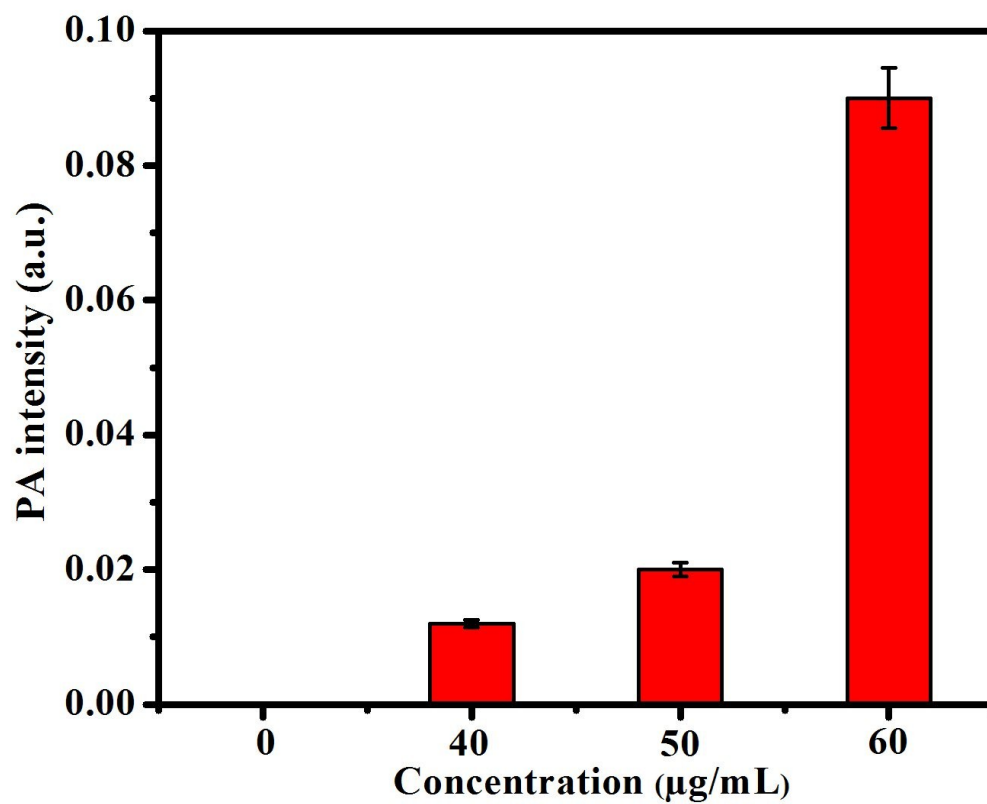


Fig. S26. Photoacoustic signals monitored in the cells with various concentrations of FA-COS-TGA-GNRs-DOX.

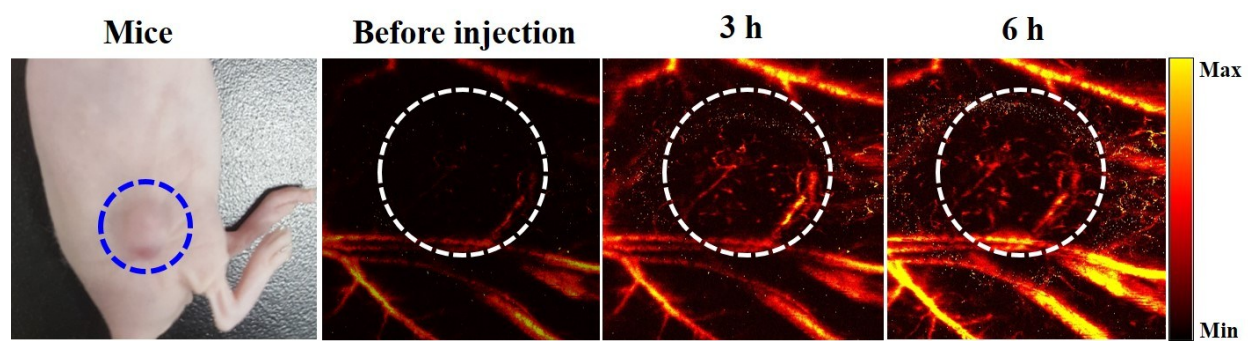


Fig. S27. *In vivo* photoacoustic images of tumor of nude mice before injection and 3 h and 6 h intravenous post-injections of FA-COS-TGA-GNRs-DOX. The white circle indicates the tumor area.

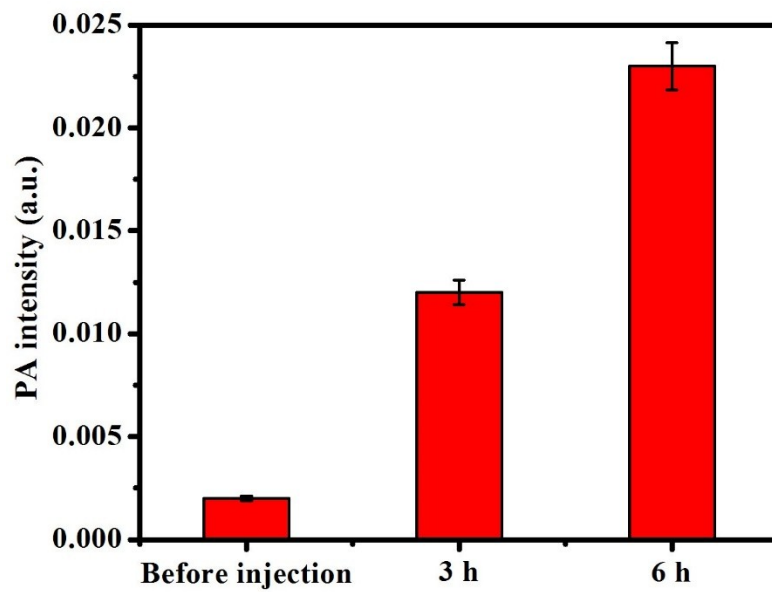


Fig. S28. The average PA signal of FA-COS-TGA-GNRs-DOX in the tumor at various time intervals.

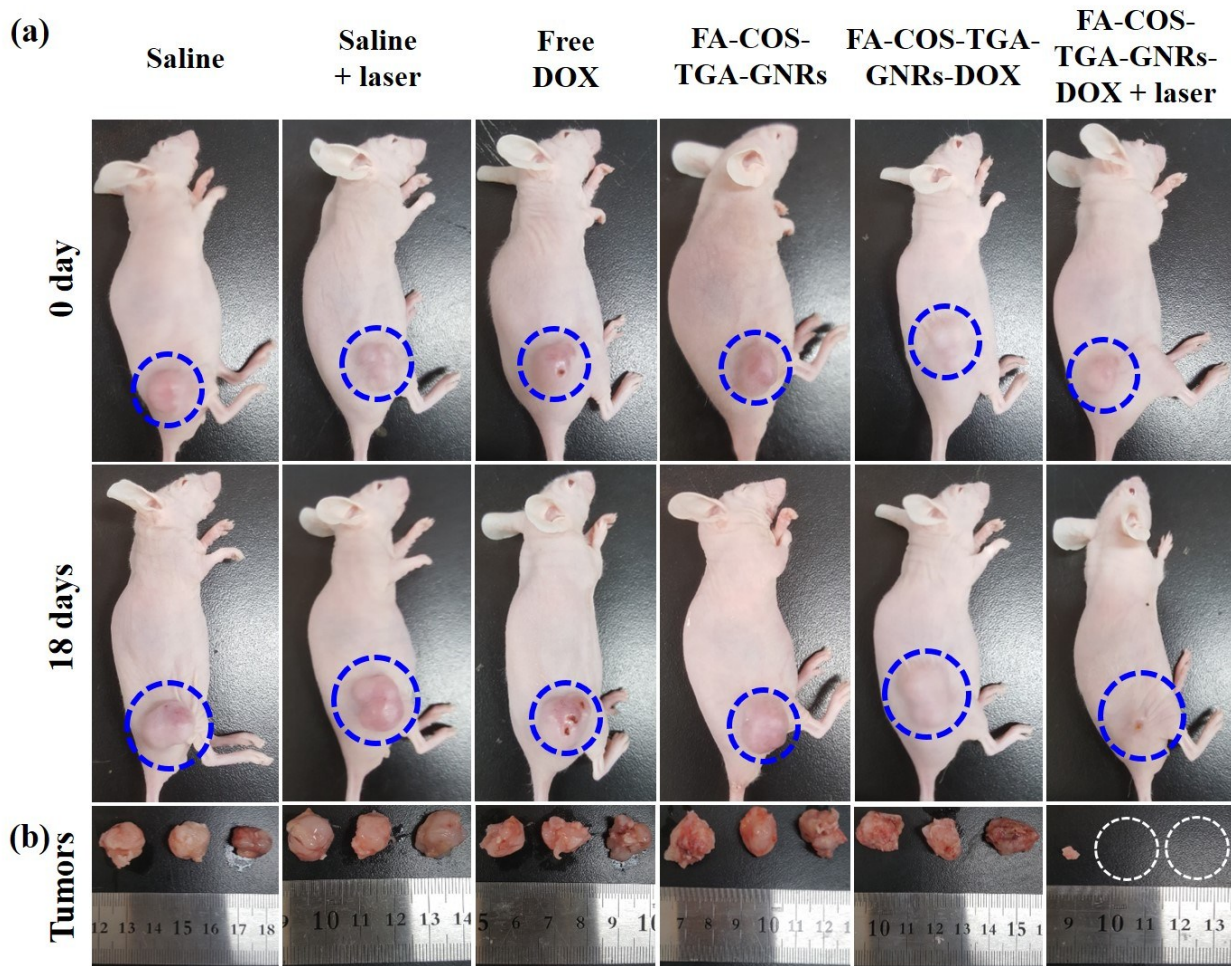


Fig. S29. (a) Representative digital photographs of MDA-MB-231 tumor-bearing mice in each group before (0 day) and after 18 days of treatments. (b) Representative digital photographs of tumors in various groups after 18 days of treatment. Data are represented as mean \pm standard derivation (SD) for the five experiments.

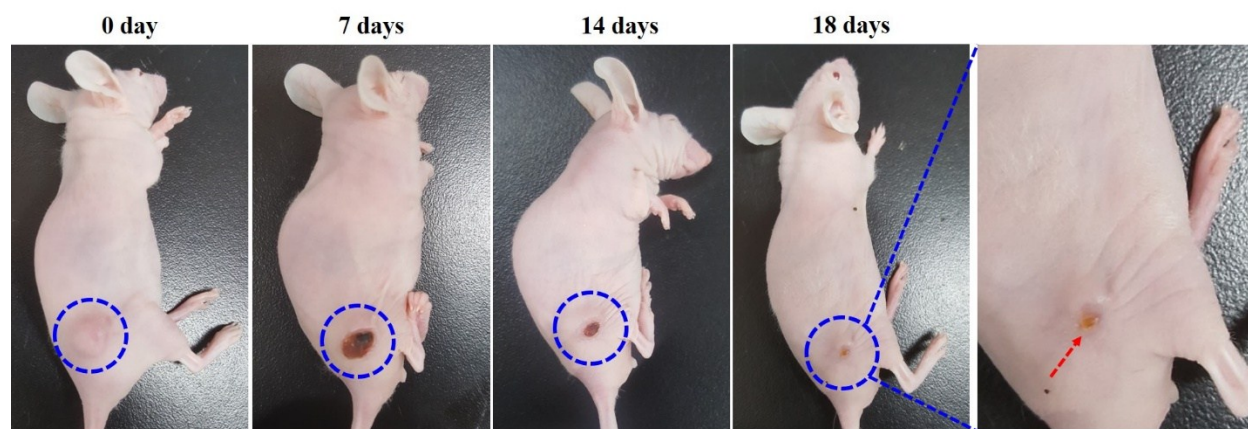


Fig. S30. The digital photographs of MDA-MB-231 tumor-bearing mice taken before treatment (0 day) and after treatment (7, 14, and 18 days) of FA-COS-TGA-GNRs-DOX under laser irradiation (1.0 W cm^{-2}) for 300 s.

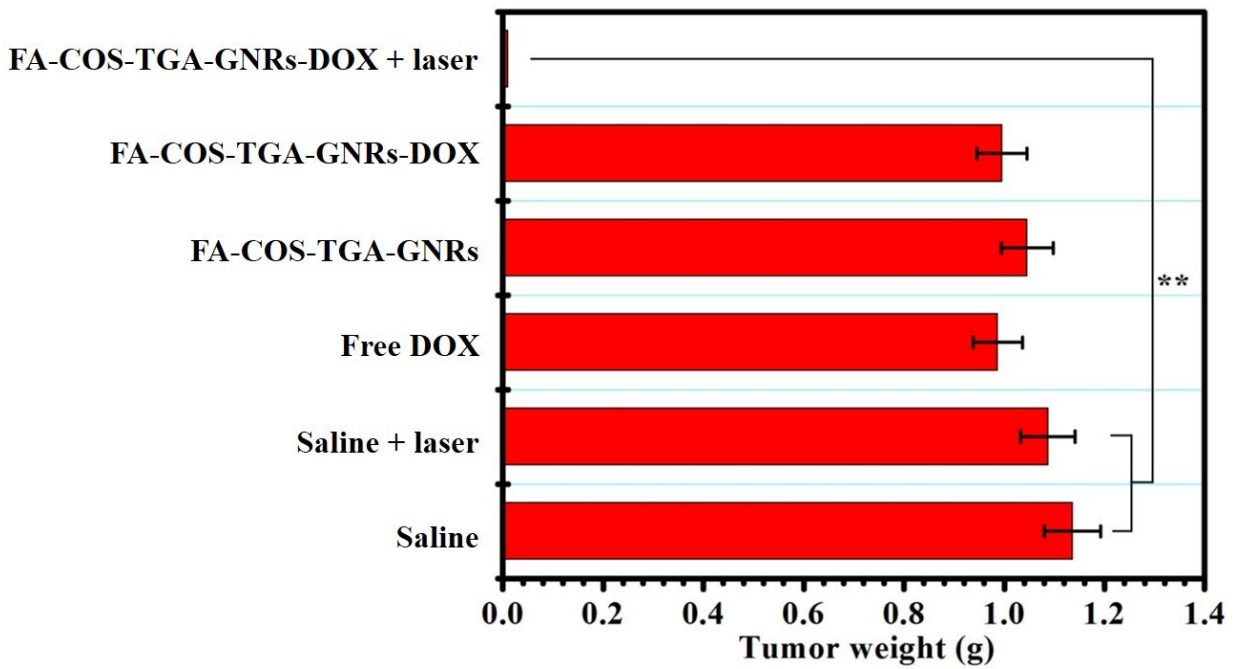


Fig. S31. The average weight of tumors collected from each group of MDA-MB-231 tumor-bearing mice after treatment. Data are represented as mean \pm standard deviation (SD) for the five experiments (** significant $p < 0.01$).

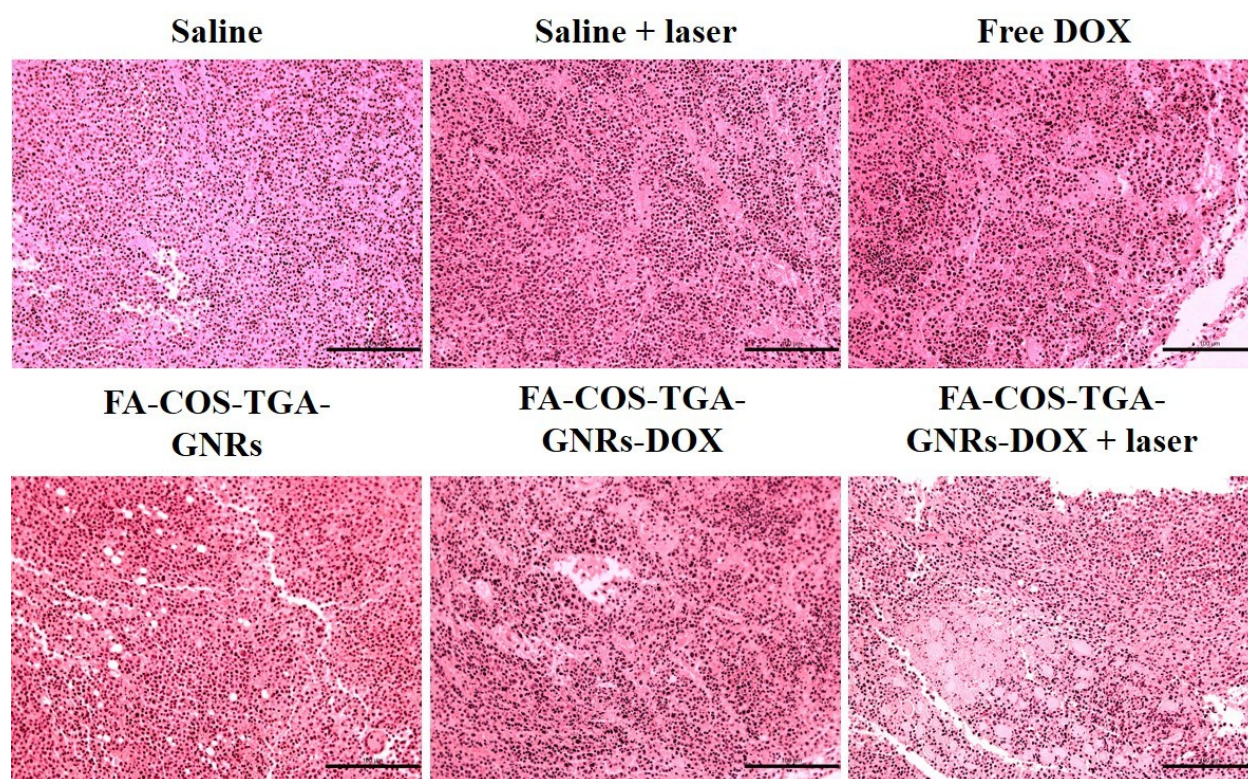


Fig. S32. Hematoxylin/eosin (H&E) staining of tumor tissues from various groups (20 × magnification). Scale bar: 100 μm.

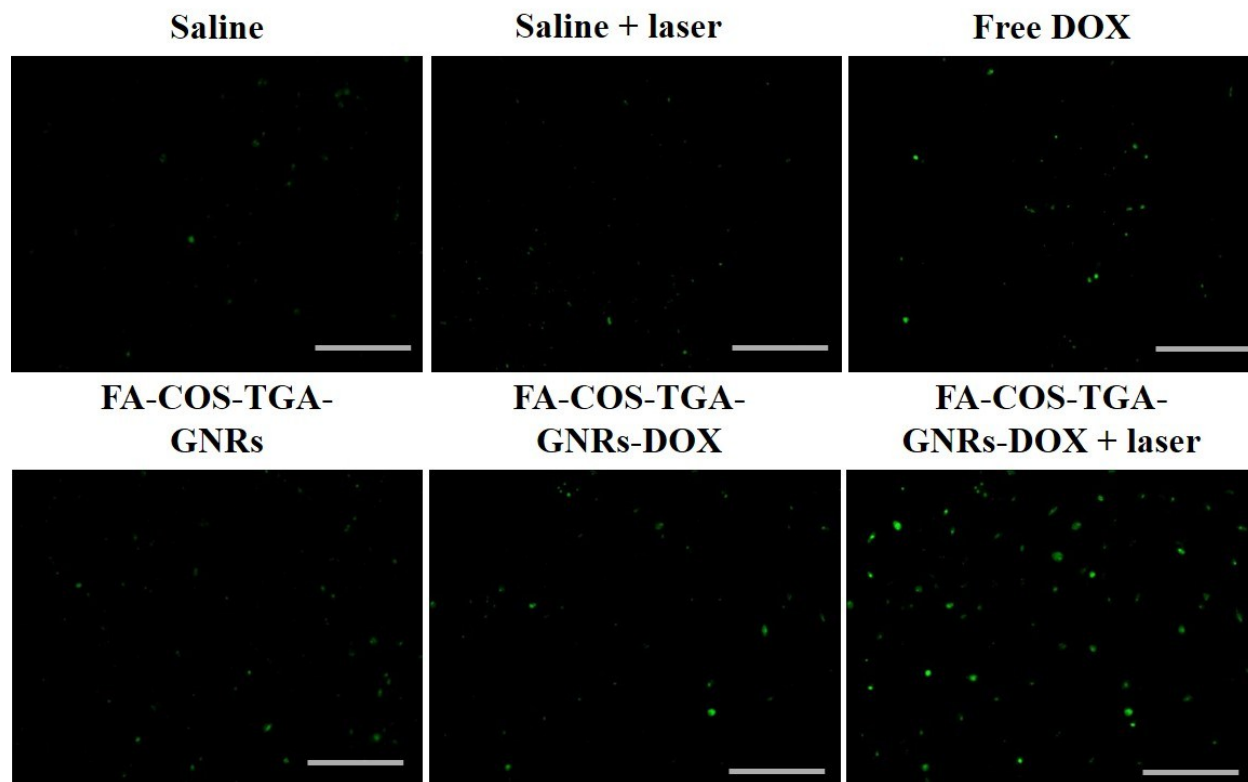


Fig. S33. TUNEL staining assay of tumors tissues after treatments. The apoptotic cells labelled green fluorescence were evidently identified by TUNEL assay ($20 \times$ magnification). Scale bar: $100 \mu\text{m}$.

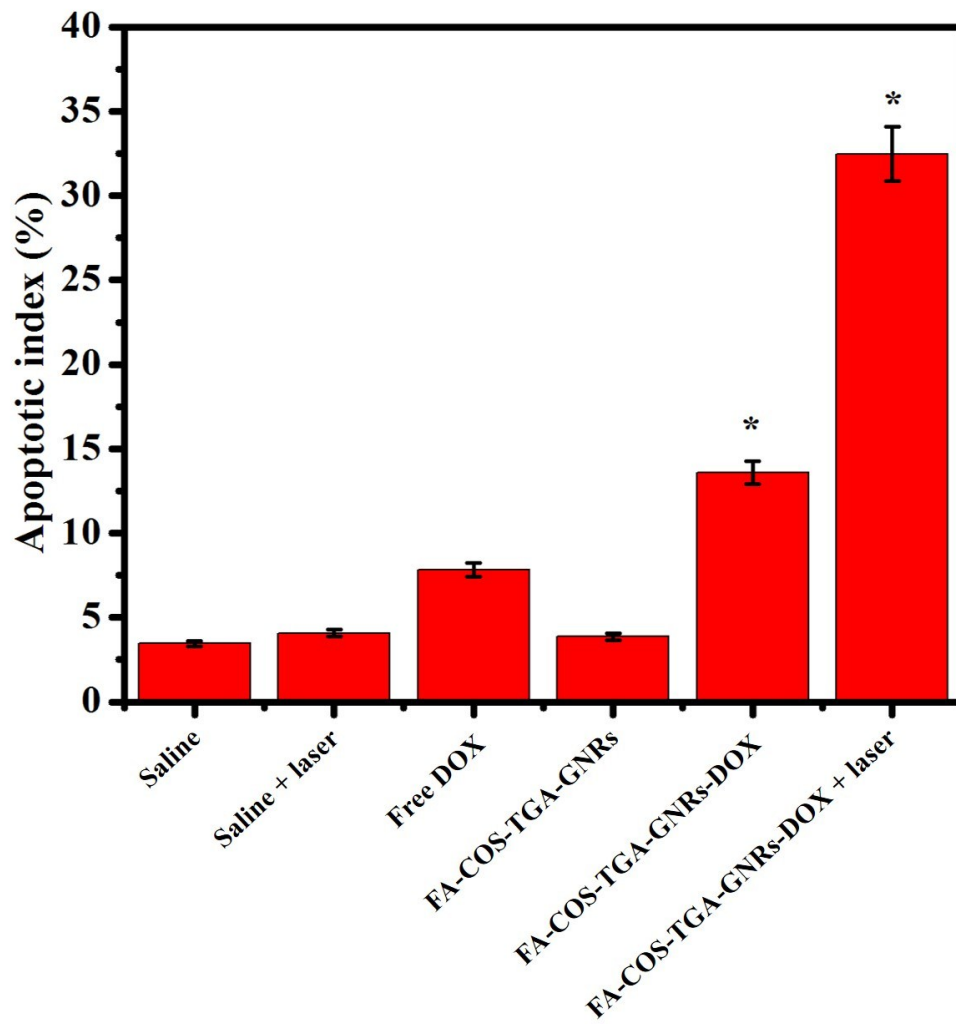


Fig. S34. The apoptotic index was observed in the PTT groups using the TUNEL assay.

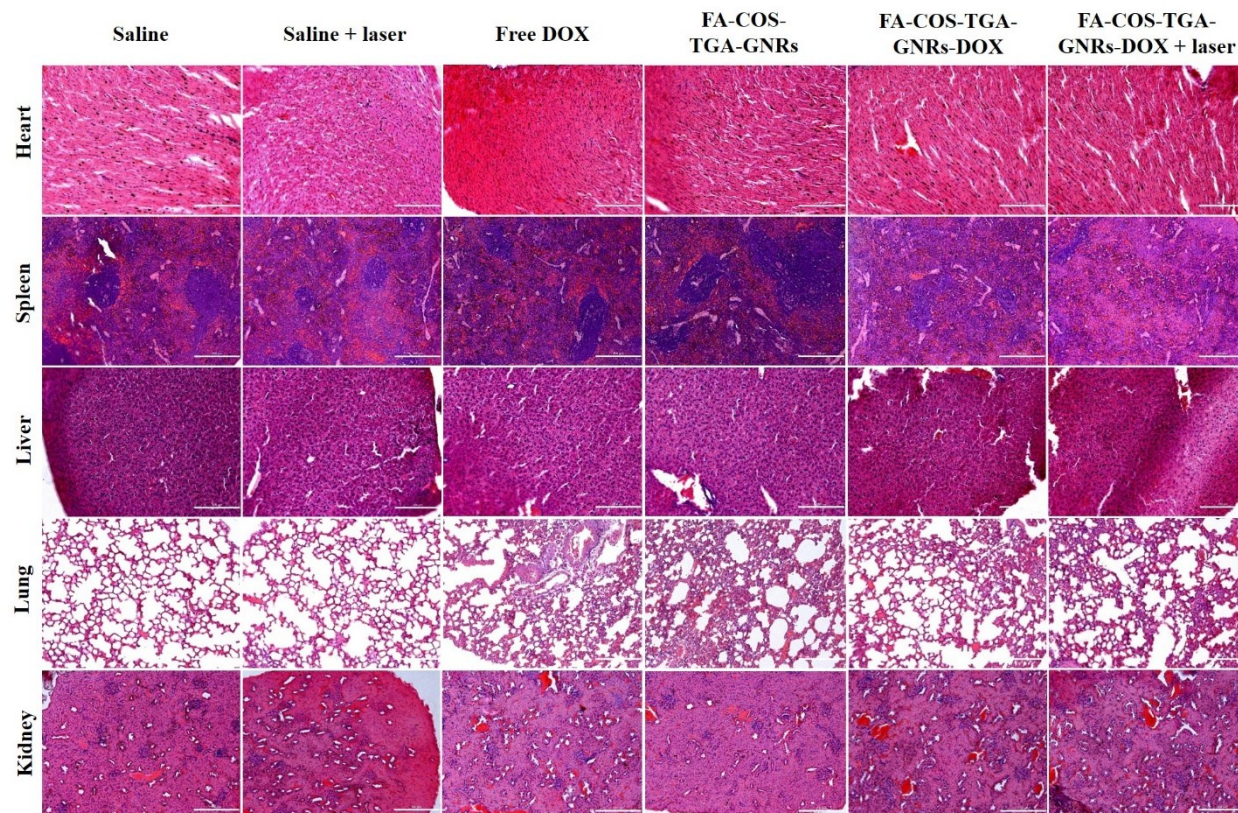


Fig. S35. H&E staining of the five main organs from various groups.

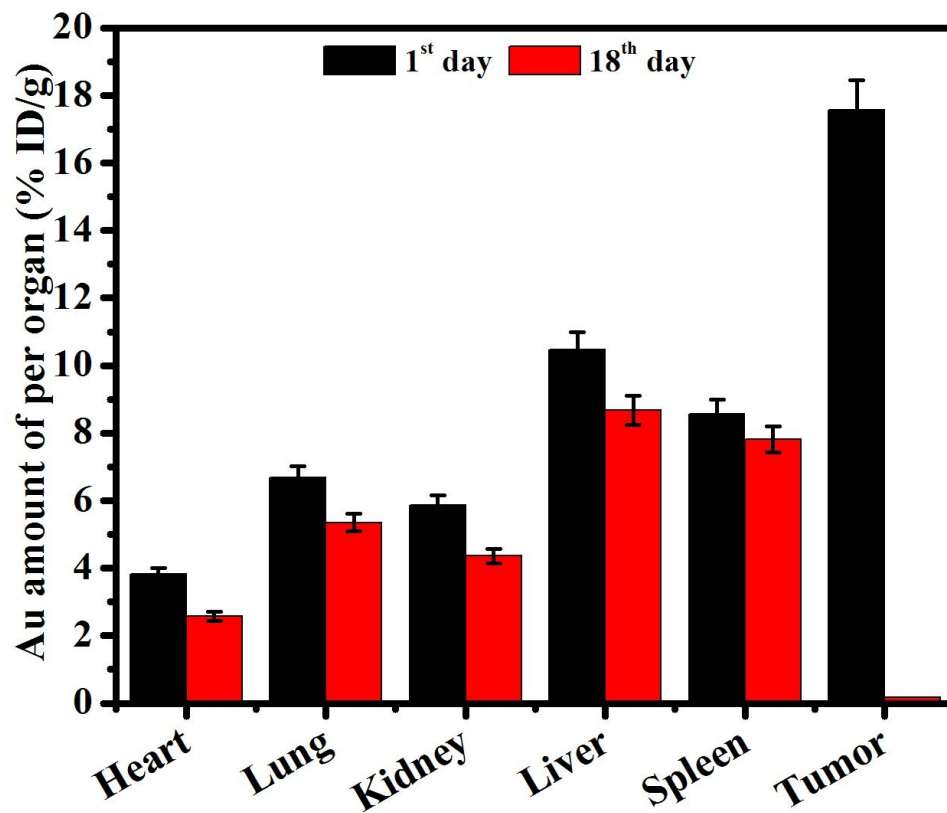


Fig. S36. The biodistribution of FA-COS-TGA-GNRs-DOX in mice on the 1st day and 18th day of treatment.

Table S1. Hematology analysis and blood biochemical assay

	Saline	FA-COS-TGA-GNRs-DOX
WBC ($10^9/L$)	5.2 ± 0.62	4.7 ± 0.68
RBC ($10^{12}/L$)	9.6 ± 0.41	9.1 ± 1.36
MCV (fl)	49.6 ± 0.78	48.5 ± 1.7
HGB (g/L)	138 ± 4.81	140 ± 5.33
PLT ($10^9/L$)	1087 ± 56	1052 ± 73
AST (U/L)	141.3 ± 6.2	139.4 ± 4.7
ALT (U/L)	48 ± 4.7	50 ± 2.8
BUN ($\mu\text{mol}/L$)	10 ± 0.4	10.1 ± 0.8
CRE (mmol/L)	6.4 ± 0.8	7.0 ± 0.5

References

1. Q. Yang, C. He, Y. Xu, B. Liu, Z. Shao, Z. Zhu, Y. Hou, B. Gong and Y.-M. Shen, *Poly. Chem.*, 2015, **6**, 1454-1464.
2. T. S. C. Li, T. Yawata and K. Honke, *Eur. J. Pharm. Sci.*, 2014, **52**, 48-61.
3. B. Nikoobakht and M. A. El-Sayed, *Chem. Mater.*, 2003, **15**, 1957-1962.
4. T. K. Sau and C. J. Murphy, *Langmuir*, 2004, **20**, 6414-6420.
5. L. Liu, Z. Guo, L. Xu, R. Xu and X. Lu, *Nanoscale Res. Lett.*, 2011, **6**, 143.
6. X. Ye, C. Zheng, J. Chen, Y. Gao and C. B. Murray, *Nano Lett.*, 2013, **13**, 765-771.
7. L. Fontana, M. Bassetti, C. Battocchio, I. Venditti and I. Fratoddi, *Colloids Surfaces A: Physicochem. Eng. Aspects.*, 2017, **532**, 282-289.
8. E. Peng, J. Ding and J. M. Xue, *J. Mater. Chem.*, 2012, **22**, 13832-13840.
9. A. Di Martino, P. Kucharczyk, Z. Capáková, P. Humpolicek and V. Sedlarik, *Int. J. Biol. Macromol.*, 2017, **102**, 613-624.
10. S. W. Jun, J. Kwon, S. K. Chun, H. A. Lee, J. Lee, D. Y. Hwang, C.-Y. Dong and C.-S. Kim, *Biomed. Opt. Express*, 2018, **9**, 705-716.
11. J. Zhang, C. Yang, R. Zhang, R. Chen, Z. Zhang, W. Zhang, S. H. Peng, X. Chen, G. Liu and C. S. Hsu, *Adv. Funct. Mater.*, 2017, **27**, 1-23.
12. D. K. Roper, W. Ahn and M. Hoepfner, *J. Phys. Chem. C*, 2007, **111**, 3636-3641.
13. X. Liu, B. Li, F. Fu, K. Xu, R. Zou, Q. Wang, B. Zhang, Z. Chen and J. Hu, *Dalton Trans.*, 2014, **43**, 11709-11715.
14. W. Yin, L. Yan, J. Yu, G. Tian, L. Zhou, X. Zheng, X. Zhang, Y. Yong, J. Li and Z. Gu, *ACS Nano*, 2014, **8**, 6922-6933.

15. R. Coradeghini, S. Gioria, C. P. García, P. Nativo, F. Franchini, D. Gilliland, J. Ponti and F. Rossi, *Toxicol. Lett.*, 2013, **217**, 205-216.
16. H. Yang, M. Xu, S. Li, X. Shen, T. Li, J. Yan, C. Zhang, C. Wu, H. Zeng and Y. Liu, *RSC Adv.*, 2016, **6**, 29685-29696.
17. M. Huang, Z. Ma, E. Khor and L.-Y. Lim, *Pharm. Res.*, 2002, **19**, 1488-1494.
18. N. Q. Bui, K. K. Hlaing, V. P. Nguyen, T. H. Nguyen, Y.-O. Oh, X. F. Fan, Y. W. Lee, S. Y. Nam, H. W. Kang and J. Oh, *Comput. Med. Imaging Graph.*, 2015, **45**, 57-62.
19. P. Manivasagan, N. Q. Bui, S. Bharathiraja, M. S. Moorthy, Y.-O. Oh, K. Song, H. Seo, M. Yoon and J. Oh, *Sci. Rep.*, 2017, **7**, 43593.